Journal of Computational Dynamics
doi:10.3934/jcd.2017003

RIGOROUS CONTINUATION OF BIFURCATION POINTS IN THE DIBLOCK COPOLYMER EQUATION

Jean-Philippe Lessard

Department of Mathematics and Statistics
McGill University
805 Sherbrooke St W
Montreal, QC, H3A 0B9, Canada

Evelyn Sander

Department of Mathematical Sciences
George Mason University
Fairfax, Virginia 22030, USA

Thomas Wanner*

Department of Mathematical Sciences
George Mason University
Fairfax, Virginia 22030, USA

(Communicated by Marian Mrozek)

Abstract. We develop general methods for rigorously computing continuous branches of bifurcation points of equilibria, specifically focusing on fold points and on pitchfork bifurcations which are forced through $\mathbb{Z}_2$ symmetries in the equation. We apply these methods to secondary bifurcation points of the one-dimensional diblock copolymer model.

1. **Introduction.** Understanding the equilibrium structure of nonlinear partial differential equations lies at the heart of many important applied problems. Unfortunately, there are no general techniques which allow one to obtain a complete answer for any such problem. In some cases, maximum principle methods can be used to obtain partial results, in other cases one can reduce the problem to studying specific connecting orbits in associated ordinary differential equations. Both of these types of methods are restricted to the case of partial differential equations on one-dimensional domains, but even in this case many answers remain elusive.

One alternative that has been developed over the last decades is the use of computer-assisted proofs in the study of equilibrium problems of nonlinear partial differential equations. Part of the allure of these methods is that they do not depend on the order of the partial differential equation. For example, in contrast to classical maximum principle methods, which cannot generally be used for fourth-order partial differential equations, rigorous computational methods have been successfully

2010 *Mathematics Subject Classification.* Primary: 35B40, 65G20, 65P30; Secondary: 35B41, 35K55, 65G30, 65N35, 74N99.

Key words and phrases. Bifurcation diagram, pitchfork bifurcations, saddle-node bifurcations, symmetry, computer assisted-proof, diblock copolymer model.

* Corresponding author: T. Wanner.

applied to the stationary Cahn-Hilliard equation [13, 22, 23], the diblock copolymer model [35, 36, 37, 38], as well as to others such as [25, 40].

Almost all equilibrium problems that arise in applications involve a number of parameters, and one is generally interested in understanding how the structure of the equilibrium set changes as these parameters are varied. In this context, precise mathematical methods from bifurcation theory exist which can predict where changes in the solution set occur, i.e., they address the location of bifurcation points. In addition, they can provide complete local descriptions of emerging solution branches. Yet, these methods usually fail to provide information on the global structure of such branches. Also in this context, rigorous computational techniques have successfully been used, see for example [2, 11, 14, 35, 31] and [1, 28, 29], where the latter group considered bifurcation points as well as solution branches.

In the current paper, we show that rigorous computational methods can locate curves in parameter space along which certain types of bifurcation points occur. Our focus is on studying secondary bifurcation points using rigorous computational techniques, including saddle-node bifurcations and symmetry-breaking pitchfork bifurcations. Our interest in this problem stems from recent work on the diblock copolymer equation, which for the one-dimensional domain $\Omega = (0, 1)$ is given by

$$\begin{aligned} u_t &= -\left(u_{xx} + \lambda f(u)\right)_{xx} - \lambda\sigma(u - \mu) \,, \qquad (1)\\ &\text{subject to the mass constraint} \quad \mu = \int_0^1 u(x)dx \,, \\ &\text{as well as} \quad u_x(x) = u_{xxx}(x) = 0 \quad \text{for} \quad x = 0, 1 \,. \end{aligned}$$

where in the following we use the nonlinearity $f(u) = u - u^3$. This partial differential equation is a model for microphase separation in diblock copolymers as described in [26]. These are formed by the reaction of two linear polymers, or blocks, containing different monomers. The function u is the relative macroscopic density of the two monomers. The parameter μ is the total mass of u. Roughly speaking, large λ represents strong short range repulsion, resulting in short range separation. Large σ indicates strong long range elasticity forces. In two and three dimensions, the interaction between the two forces results in the formation of special geometries, which induce patterns such as spots, stripes, and gyroids. In its original form it was proposed by Ohta and Kawasaki [27] and Bahiana and Oono [3]. For more information regarding its derivation and the involved parameters we refer the reader to Choksi and Ren [8, 9].

In [17] we combined rigorous bifurcation-theoretic results with numerical simulations to shed light on the long-term dynamics of the diblock copolymer model in one dimension. It is well-known that the model exhibits multi-stability, i.e., the coexistence of multiple stable equilibrium solutions. Furthermore, the constant function $u \equiv \mu$ is always an equilibrium solution for the diblock copolymer model, representing a homogeneous polymer blend. For sufficiently large values of the parameter λ this stationary state loses its stability, and one is generally interested in the long-term behavior of solutions of (1) which originate close to μ. It was shown in [17] that the spatial periodicity of the long-term limit of typical solutions changes along well-defined curves in the λ-σ-parameter plane. In fact, numerical path-following computations suggested that these curves are the locations of very specific secondary bifurcation points in the diblock copolymer bifurcation diagram.

The diblock copolymer model is a regular perturbation, with respect to the pa-

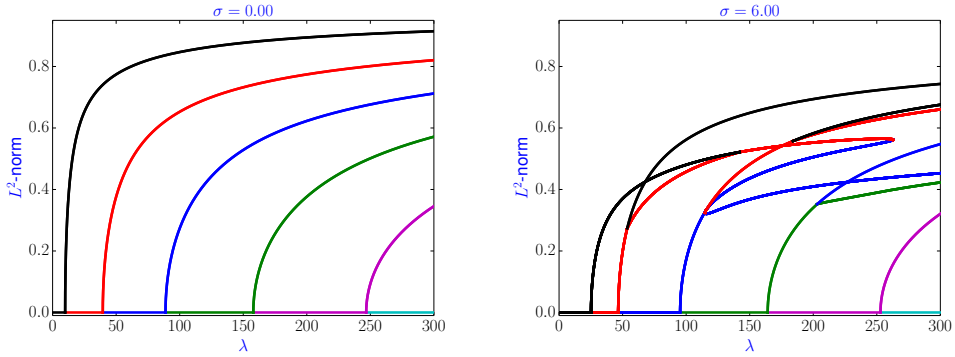

FIGURE 1. Equilibrium bifurcation diagrams of the Cahn-Hilliard model (left image) and the diblock copolymer model for $\sigma = 6$ (right image). In both figures, $\mu = 0$. Most of the shown branches actually correspond to two or more solution branches, since the L^2-norm of the associated solutions is used as the vertical diagram axis. The colors correspond to the indices of the solutions. Along the horizontal trivial solution branch they increase from zero (black) to five (cyan).

rameter σ, of the standard Cahn-Hilliard model, which corresponds to $\sigma = 0$. The equilibrium structure of the Cahn-Hilliard equation has been completely described by Grinfeld & Novick-Cohen [15] by combining phase-plane analysis with transversality arguments, and this leads to a bifurcation diagram as in the left image of Figure 1. The method of [15] relies on the fact that the stationary Cahn-Hilliard problem in one dimension can be integrated twice, reducing it to a second-order nonlinear boundary value problem. However, this is no longer the case in the diblock copolymer model — which is certainly responsible for the fact that our knowledge of its equilibrium structure is extremely limited. Nevertheless, as a regular perturbation problem the bifurcation diagram of the Cahn-Hilliard model changes in a continuous manner as σ is increased from zero. Part of this change was discussed in [17]. Namely, it was shown that as σ increases from zero, there is an infinite sequence of branch interactions near the trivial solution line as the branches successively move to the right. These local interactions have been rigorously described in [17] using analytical bifurcation-theoretic techniques. Further, the local bifurcations are observed to combine with global bifurcations from infinity, leading to different types of branch interactions at secondary bifurcations. Five of these secondary bifurcation points can be seen in the right image of Figure 1, which shows part of the diblock copolymer bifurcation diagram for $\sigma = 6$. While one of these points is a regular saddle-node type bifurcation point, the remaining four are of pitchfork type. Understanding the locations of these secondary bifurcation points in the λ-σ-parameter plane lies at the heart of understanding how the complicated diblock copolymer bifurcation diagram is obtained from the simple Cahn-Hilliard diagram. For more details, we refer the reader to the survey [37].

Motivated by the above discussion, in this paper we develop a rigorous computational method to compute the location curves of secondary bifurcation points as above. For the case of the saddle-node type bifurcation point this is accomplished

by considering a standard extended system which encodes both the existence condition for the equilibrium point and the existence of a one-dimensional non-degenerate kernel of the linearization of the diblock copolymer model at this equilibrium. This extended system will lead to a well-defined continuation problem. However, for the remaining four secondary bifurcation points in the right image of Figure 1 this extended system has a degeneracy. This is due to the fact that these bifurcation points are pitchfork bifurcations which are forced by symmetries in the model. In these cases we employ a method due to Werner & Spence [39] to derive a well-defined continuation problem. While in this paper we concentrate on the case of the diblock copolymer model, similar questions arise in the study of nucleation in the Cahn-Hilliard model, as described in [4, 5, 6, 12]. In this paper, we develop a generally applicable method for solving problems with saddle-node bifurcations and $\mathbb{Z}_2$ symmetry-breaking pitchfork bifurcations. While we only apply this method in the context of the diblock copolymer equation (with $\mu = 0$ chosen in order to allow for antisymmetric solutions), the method is directly applicable in a broad range of applications. In addition, we believe that the method can be extended to symmetry-breaking bifurcations for other symmetry classes.

After developing the general functional analytic method for rigorously verifying the existence of bifurcation points, we apply it in several specific secondary bifurcations for the one-dimensional diblock copolymer model. We do so using the method of radii polynomials. In this context, we write everything in terms of the Banach space of Fourier series. We then use a series of previously established estimates on the functional manipulation of such series. This allows us to be able to handle the rigorous estimates on the infinite-dimensional function space.

Our final results using the radii polynomial techniques consist of a set of three validated branches of saddle-node bifurcations and three validated branches of symmetry-breaking pitchfork bifurcations. Each of these cases were found numerically in [17], where it was observed numerically that there was scaling law of different bifurcation branches. From the point of view of the general techniques of the first part of this paper, these results serve as a proof of concept. From the point of view of better understanding the diblock copolymer equations, the validation of these branches of bifurcations is a first step, where our eventual goal is to combine such results with analytical methods in order to validate the scalings of bifurcation branches that we observed in the previous paper.

The remainder of the paper is organized as follows. In Section 2 we present the functional-analytic setting for our studies, showing how the results of [39] can be adapted to our situation. In Section 2.1 we view the set of equilibria of a differential equation as the zero set of a nonlinear mapping in an abstract function space. We use the Lyapunov-Schmidt reduction technique to study the zero set of such a mapping. This section includes the introduction of equivariant symmetry, with the goal of being able to treat symmetry-breaking bifurcations. In Section 2.2, we then apply the Lyapunov-Schmidt method to saddle-node bifurcations. We introduce an extended system consisting of the nonlinear mapping whose zero set consists of equilibria, along with two other bifurcation conditions. We then apply our abstract approach to the extended system to prove the existence of saddle-node bifurcation points. Finally, in 2.3, we treat the case of pitchfork bifurcations. This time we make assumptions of equivariance of the nonlinear mapping, and the existence of a solution which is either symmetric or antisymmetric. This allows us to prove the existence of symmetry-breaking pitchfork bifurcation points. In Section 2.4, we

demonstrate that the diblock copolymer equation satisfies all the assumptions necessary for our abstract setting. Section 3 gives specific details of how to transfer the abstract functional-analytic existence results into a rigorous computational method. In particular, we give existence results for equilibrium solutions at regular and bifurcation points, where our solutions are proved to be contained in a precisely defined small neighborhood of a function given in the form of a truncated Fourier series expansion. Section 3.1 gives the function-analytic background for rigorous bounds on manipulated functions given in terms of Fourier series expansions. Section 3.2 details the method of sequentially validating the curve of equilibrium solutions of the equation as a parameter is varied using the radii polynomial approach. Section 3.3 and Section 3.4 provide the detailed estimates and the bounds required to define the radii polynomial associated to the saddle-node bifurcations and respectively to the pitchfork bifurcations. Finally, in Section 3.5, the radii polynomial approach is combined with the Lyapunov-Schmidt results in Section 2 in order to establish branches of saddle-node and pitchfork bifurcations for the diblock copolymer equation.

2. Extended systems for locating bifurcation points.

In this section we present the functional-analytic framework which will be used to study the continuation of bifurcation points using rigorous computational techniques. As we anticipate that our methods are applicable to a wide variety of settings, we formulate the results first in a general Banach space setting, and apply them only later to the diblock copolymer model. We note that a number of these results are standard, but we include a brief version of the proofs for completeness in the efforts of keeping the paper self-contained, as well as to set the results into our notation.

2.1. Lyapunov-Schmidt reduction and equivariance.

We begin by recalling the basic functional-analytic tool which can be used to study the equilibrium set of nonlinear equations in Banach spaces — the Lyapunov-Schmidt reduction. The results of this section are all well-known and stated only to keep the presentation as self-contained as possible. For more details we refer the reader to [10, 41]. We study nonlinear operator equations of the form

$$F(\lambda, u) = 0\,, \tag{2}$$

where $F : \mathbb{R} \times X \to Y$ is a smooth nonlinear mapping, and X and Y are real Banach spaces. Throughout this section, we assume the following.

Assumption 2.1 (Fredholm Property)**.** *Let X and Y denote real Banach spaces, and assume that the parameter-dependent nonlinear operator $F : \mathbb{R} \times X \to Y$ is sufficiently smooth. Suppose that the point (λ_0, u_0) is a solution of (2), i.e., that we have the identity $F(\lambda_0, u_0) = 0$. Finally, we assume that the Fréchet derivative $L = D_u F(\lambda_0, u_0) \in \mathcal{L}(X, Y)$ is a Fredholm operator of index zero.*

In addition, we will only consider possible bifurcation points which exhibit a one-dimensional nullspace. This leads to the following second assumption.

Assumption 2.2 (One-Dimensional Kernel)**.** *Suppose that Assumption 2.1 holds. Assume further that the linearization $L = D_u F(\lambda_0, u_0)$ has a one-dimensional kernel. Since it has index zero, its range has co-dimension one. In this case, we have*

$$N(L) = \operatorname{span}[\varphi_0] \quad \text{and} \quad R(L) = N(\psi_0^*)$$

for some nonzero elements $\varphi_0 \in X$ and $\psi_0^* \in Y^*$, where Y^* denotes the dual space of Y. Finally, let $\tilde{X} \subset X$ and $\tilde{Y} \subset Y$ denote closed subspaces such that

$$X = N(L) \oplus \tilde{X} \qquad \text{and} \qquad Y = \tilde{Y} \oplus R(L) \ ,$$

where the continuous linear projector $P : Y \to Y$ is defined via the two identities $R(P) = \tilde{Y}$ and $N(P) = R(L)$, while the projector $Q : X \to X$ is defined via $R(Q) = N(L)$ and $N(Q) = \tilde{X}$. Notice that both P and Q have rank one.

In the above situation, one can study the solution set of (2) in a neighborhood of (λ_0, u_0) by solving an associated real-valued equation which involves only two real arguments, the so-called bifurcation equation. It is the subject of the following proposition which describes the Lyapunov-Schmidt reduction.

Proposition 2.3 (Lyapunov-Schmidt Reduction)**.** *In the situation of Assumptions 2.1 and 2.2 there exist a neighborhood Λ_0 of λ_0, a neighborhood V_0 of $v_0 = Qu_0 \in N(L)$, a smooth function $W : \Lambda_0 \times V_0 \to \tilde{X}$, as well as a smooth real-valued function b which is defined in a neighborhood of the point $(\lambda_0, 0) \in \mathbb{R}^2$ such that the following hold:*

(a) If (λ, α) is sufficiently close to the point $(\lambda_0, 0) \in \mathbb{R}^2$ and satisfies $b(\lambda, \alpha) = 0$, then we have

$$F(\lambda, u) = 0 \quad \text{for} \quad u = v_0 + \alpha\varphi_0 + W\left(\lambda, v_0 + \alpha\varphi_0\right) \ .$$

(b) Conversely, if (λ, u) is close enough to (λ_0, u_0) and solves $F(\lambda, u) = 0$, then for α defined via $v_0 + \alpha\varphi_0 = Qu$ we have $b(\lambda, \alpha) = 0$ and $u = Qu + W(\lambda, Qu)$.

In other words, the solution set of $b(\lambda, \alpha) = 0$ in a neighborhood of $(\lambda_0, 0) \in \mathbb{R}^2$ is in one-to-one correspondence to the solution set of $F(\lambda, u) = 0$ in a neighborhood of the point (λ_0, u_0).

Proof. According to Assumption 2.2, solving the nonlinear problem (2) is equivalent to solving the two equations

$$PF(\lambda, v + w) = 0 \ , \qquad \text{as well as} \tag{3}$$

$$(I - P)F(\lambda, v + w) = 0 \ . \tag{4}$$

where $v = Qu$ and $w = (I - Q)u$. If we define $G(\lambda, v, w) = (I - P)F(\lambda, v + w)$, then our assumptions readily imply that $G : \mathbb{R} \times N(L) \times \tilde{X} \to R(L)$. If we further introduce the abbreviations $v_0 = Qu_0$ and $w_0 = (I - Q)u_0$, then $G(\lambda_0, v_0, w_0) = 0$, and

$$D_w G(\lambda_0, v_0, w_0) = (I - P)L|_{\tilde{X}} = L|_{\tilde{X}} \in \mathcal{L}\left(\tilde{X}, R(L)\right) \ .$$

According to our definition of $\tilde{X}$ the continuous linear operator $D_w G(\lambda_0, v_0, w_0)$ is therefore one-to-one and onto, hence continuous with continuous inverse — and one can apply the implicit function value theorem to solve (4) locally for w as a function of λ and v. This furnishes the function W as in the formulation of the theorem. Plugging W into (3) shows that locally near (λ_0, u_0) a pair (λ, u) solves $F(\lambda, u) = 0$ if and only if $(\lambda, v) = (\lambda, Qu)$ satisfies

$$PF\left(\lambda, v + W(\lambda, v)\right) = 0 \ .$$

If we now set $b(\lambda, \alpha) = \psi_0^*(PF(\lambda, v_0 + \alpha\varphi_0 + W(\lambda, v_0 + \alpha\varphi_0)))$, then the result follows due to our choices of ψ_0^* and P. □

$$
\begin{aligned}
D_\lambda b(\lambda_0,0) &= \psi_0^* D_\lambda F(\lambda_0,u_0)\ ,\\
D_{\lambda\alpha} b(\lambda_0,0) &= \psi_0^* D_{\lambda u} F(\lambda_0,u_0)[\varphi_0]\\
&\quad + \psi_0^* D_{uu} F(\lambda_0,u_0)[\varphi_0, D_\lambda W(\lambda_0,v_0)]\ ,\\
D_{\alpha\alpha} b(\lambda_0,0) &= \psi_0^* D_{uu} F(\lambda_0,u_0)[\varphi_0,\varphi_0]\ ,\\
D_{\alpha\alpha\alpha} b(\lambda_0,0) &= \psi_0^* D_{uuu} F(\lambda_0,u_0)[\varphi_0,\varphi_0,\varphi_0]\\
&\quad + 3\psi_0^* D_{uu} F(\lambda_0,u_0)[\varphi_0, D_{vv} W(\lambda_0,v_0)[\varphi_0,\varphi_0]]\ ,\\
LD_\lambda W(\lambda_0,v_0) &= -(I-P) D_\lambda F(\lambda_0,u_0)\ ,\\
LD_{vv} W(\lambda_0,v_0)[\varphi_0,\varphi_0] &= -(I-P) D_{uu} F(\lambda_0,u_0)[\varphi_0,\varphi_0]\ .
\end{aligned}
$$

TABLE 1. Some of the partial derivatives of the bifurcation function $b(\lambda,\nu)$ at the point $(\lambda_0,0)$ up to order three, together with the required partial derivatives of W.

Important for applications is the fact that one can easily derive a Taylor expansion for the bifurcation function $b(\lambda,\alpha)$ near the point $(\lambda_0,0)$. One can show that

$$
\begin{aligned}
b(\lambda_0+\nu,\alpha) = \nu\cdot D_\lambda b(\lambda_0,0) &+ \frac{\nu^2}{2}\cdot D_{\lambda\lambda} b(\lambda_0,0) + \alpha\nu\cdot D_{\lambda\alpha} b(\lambda_0,0)\\
&+ \frac{\alpha^2}{2}\cdot D_{\alpha\alpha} b(\lambda_0,0) + \frac{\nu^3}{6}\cdot D_{\lambda\lambda\lambda} b(\lambda_0,0)\\
&+ \frac{\alpha\nu^2}{2}\cdot D_{\lambda\lambda\alpha} b(\lambda_0,0) + \frac{\alpha^2\nu}{2}\cdot D_{\lambda\alpha\alpha} b(\lambda_0,0)\\
&+ \frac{\alpha^3}{6}\cdot D_{\alpha\alpha\alpha} b(\lambda_0,0) + R(\nu,\alpha) \qquad (5)
\end{aligned}
$$

with $R(\nu,\alpha) = O(\|(\nu,\alpha)\|^4)$, where the derivatives of b can be computed explicitly as in Table 1, which also contains the necessary derivatives of W. Notice that the latter derivatives are all obtained through solving an inhomogeneous linear equation which involves the restriction of L onto $\tilde{X}$, which in this case is an invertible mapping.

The method of Lyapunov-Schmidt is one ingredient for our rigorous computational study of bifurcation points in the diblock copolymer equation. In order to treat pitchfork bifurcation points, we also make use of symmetry methods. For the purposes of this paper, we assume that symmetry occurs in the following specific form.

Definition 2.4 ($\mathbb{Z}_2$-Equivariance)**.** In the situation of Assumption 2.1, suppose there exist bounded linear operators $S_X \in \mathcal{L}(X)$ and $S_Y \in \mathcal{L}(Y)$ such that

$$
S_X \neq I\ ,\quad S_Y \neq I\ ,\quad S_X^2 = I\ ,\quad S_Y^2 = I\ ,
$$

as well as

$$
F(\lambda, S_X u) \;=\; S_Y F(\lambda,u) \quad \text{for all} \quad \lambda\in\mathbb{R} \quad \text{and} \quad u\in X\ . \qquad (6)
$$

Then we say that F is $\mathbb{Z}_2$-*equivariant*. Based on the symmetry operators S_X and S_Y one can also decompose the underlying Banach spaces into the *symmetric elements*

and the *antisymmetric elements*. More precisely, for the Banach space X we define

$$X_s = \{u \in X \ : \ S_X u = u\} \qquad \text{and} \qquad X_a = \{u \in X \ : \ S_X u = -u\} \ ,$$

and analogously one can define the subspaces Y_s and Y_a of Y. Then it is straightforward to show that

$$X = X_s \oplus X_a \qquad \text{as well as} \qquad Y = Y_s \oplus Y_a \ .$$

In our applications below, the operators S_X and S_Y are usually given by the same formula, even though they act on different Banach spaces. We therefore simply drop the subscripts in the following to simplify notation. It will always be clear from context whether S acts on X or on Y.

For the nonlinear equation (2), equivariance has immediate consequences regarding invariance of subspaces, both for the equation and for certain derivatives of F. For example, by differentiating the identity (6) with respect to u one immediately obtains

$$D_u F\left(\lambda, S_X u\right)\left[S_X v\right] = S_Y D_u F\left(\lambda, u\right)\left[v\right] \tag{7}$$

for all $\lambda \in \mathbb{R}$ and $u, v \in X$. If one assumes in addition $v \in X_s$, then (7) furnishes the $\mathbb{Z}_2$-equivariance of the Fréchet derivative $D_u F(\lambda, u)$. The following lemma collects a number of similar properties, which will be useful later on. The results are stated without their straightforward proofs, see also [39].

Lemma 2.5 (Equivariance of Partial Derivatives)**.** *Suppose that Assumption 2.1 holds, and that (2) is $\mathbb{Z}_2$-equivariant as in Definition 2.4. Then the following statements hold for all parameters $\lambda \in \mathbb{R}$, as long as we have $u \in X_s$:*

(a) We have both $F(\lambda, u) \in Y_s$ and $D_\lambda F(\lambda, u) \in Y_s$.
(b) Both the inclusions $D_u F(\lambda, u)[X_s] \subset Y_s$ and $D_u F(\lambda, u)[X_a] \subset Y_a$ are satisfied, as well as $D_{\lambda u} F(\lambda, u)[X_s] \subset Y_s$ and $D_{\lambda u} F(\lambda, u)[X_a] \subset Y_a$.
(c) The inclusions $D_{uu} F(\lambda, u)[X_s, X_s] \subset Y_s$ and $D_{uu} F(\lambda, u)[X_a, X_a] \subset Y_s$ hold, as well as $D_{uu} F(\lambda, u)[X_s, X_a] \subset Y_a$.

The above lemma applies to the derivatives of F at any point (λ, u), as long as $u \in X_s$. If we consider in particular the point (λ_0, u_0) from Assumption 2.2, even more can be said. The following result shows that both the eigenfunction φ_0 and the element ψ_0^* are symmetric or antisymmetric. In addition, the complements $\tilde{X}$ and $\tilde{Y}$ in Assumption 2.2 can be chosen such that they respect the symmetry operations as well. Note that while most of the following result is contained in the work of Werner and Spence, we were unable to find a full treatment of the details of the symmetry preservation under linear mapping as stated below.

Lemma 2.6 (Equivariance Effects of a One-Dimensional Kernel)**.** *Suppose that Assumption 2.2 holds, that (2) is $\mathbb{Z}_2$-equivariant as in Definition 2.4, and that $u_0 \in X_s$. Then the following hold:*

(a) The eigenfunction φ_0 which spans the nullspace $N(L)$ of $L = D_u F(\lambda_0, u_0)$ is either an element of X_s or of X_a, i.e., we have $S_X \varphi_0 = \varepsilon_X \varphi_0$ for some $\varepsilon_X \in \{\pm 1\}$.
(b) The element ψ_0^* which characterizes $R(L)$ is either symmetric or antisymmetric with respect to the equivariance S_Y^*, i.e., we have $S_Y^* \psi_0^* = \varepsilon_Y \psi_0^*$ for some $\varepsilon_Y \in \{\pm 1\}$.
(c) If in (b) we have $\varepsilon_Y = +1$, then the image $L[X_s]$ has codimension one in the symmetric space Y_s, and $L[X_a] = Y_a$. In contrast, if $\varepsilon_Y = -1$, then $L[X_s] = Y_s$, and the image $L[X_a]$ has codimension one in the antisymmetric space Y_a.

(d) The projectors P and Q in Assumption 2.2 can be chosen in such a way that they commute with the symmetry actions, i.e., such that $S_Y P = P S_Y$ and $S_X Q = Q S_X$.

Proof. According to Lemma 2.5(b) we have both $LX_s \subset Y_s$ and $LX_a \subset Y_a$, i.e., the splitting into symmetric and antisymmetric elements is respected by L. One can then easily see that

$$\varphi_0 = \varphi_{0,s} + \varphi_{0,a} \in X_s \oplus X_a \quad \text{if} \quad \varphi_{0,s} = \frac{\varphi_0 + S_X\varphi_0}{2} \quad \text{and} \quad \varphi_{0,a} = \frac{\varphi_0 - S_X\varphi_0}{2} \, .$$

This splitting furnishes $0 = L\varphi_0 = L\varphi_{0,s} + L\varphi_{0,a}$, and therefore $L\varphi_{0,s} = -L\varphi_{0,a}$, which in turn implies that both $L\varphi_{0,s}$ and $L\varphi_{0,a}$ are contained in $X_s \cap X_a = \{0\}$. Combining these results, both $\varphi_{0,s}$ and $\varphi_{0,a}$ are in $N(L)$, hence multiples of φ_0. Together this implies that either we have $\varphi_0 \in X_s$ or $\varphi_0 \in X_a$, which is equivalent to $S_X\varphi_0 = \varphi_0$ or $S_X\varphi_0 = -\varphi_0$, respectively. This completes the proof of (a).

In order to establish (b), note that since L is a Fredholm operator of index zero with one-dimensional nullspace, the same is true for its adjoint operator L^*, and the closed range theorem then implies that $N(L^*) = \operatorname{span}[\psi_0^*]$. The equivariance identity $S_Y L = L S_X$ immediately gives $S_X^* L^* = L^* S_Y^*$. As above, one obtains $L^* Y_s^* \subset X_s^*$ and $L^* Y_a^* \subset X_a^*$, if the symmetric and antisymmetric elements in the dual spaces are defined via the adjoints S_Y^* and S_X^*. The remainder of the proof of (b) proceeds completely analogous to the proof of (a) above.

We now turn our attention to (c). If we assume that both $L[X_s] = Y_s$ and $L[X_a] = Y_a$ are satisfied, then one can easily see that $L[X] = L[X_s \oplus X_a] = Y_s \oplus Y_a = Y$. This, however, contradicts the fact that the range $R(L)$ has codimension one in Y. In other words, we necessarily have $Y_s \setminus L[X_s] \neq \emptyset$ or $Y_a \setminus L[X_a] \neq \emptyset$, or both.

Now let ψ_0 denote an arbitrary element in $(Y_s \setminus L[X_s]) \cup (Y_a \setminus L[X_a]) \neq \emptyset$. Since $\psi_0 \neq 0$ and $\psi_0 \notin R(L)$ we can assume without loss of generality that this element is scaled in such a way that $\psi_0^*(\psi_0) = 1$. In addition, due to $\psi_0 \in Y_s \cup Y_a$ there exists a sign $\kappa \in \{\pm 1\}$ such that $S_Y\psi_0 = \kappa\psi_0$. Then one obtains

$$\kappa = \psi_0^*(\kappa\psi_0) = \psi_0^*(S_Y\psi_0) = (S_Y^*\psi_0^*)(\psi_0) = \varepsilon_Y \psi_0^*(\psi_0) = \varepsilon_Y \, ,$$

i.e., we have $S_Y\psi_0 = \varepsilon_Y\psi_0$.

Now assume $\varepsilon_Y = 1$. Then the above arguments readily show that $Y_a \setminus L[X_a] = \emptyset$, and this in turn implies $Y_s \setminus L[X_s] \neq \emptyset$. Therefore, the subspace $L[X_s]$ has codimension one in Y_s, and $L[X_a] = Y_a$. The case $\varepsilon_Y = -1$ can be treated analogously and leads to the opposite configuration.

It remains to establish (d), and we begin with the statement concerning the projection P. As in the proof of (c), let ψ_0 denote an arbitrary element in $(Y_s \setminus L[X_s]) \cup (Y_a \setminus L[X_a]) \neq \emptyset$, and we can again assume without loss of generality that $\psi_0^*(\psi_0) = 1$. In addition, one automatically obtains $S_Y\psi_0 = \varepsilon_Y\psi_0$. Now define $\tilde{Y} = \operatorname{span}[\psi_0]$, and let P be the associated projector as in Assumption 2.2. Then $Py = \psi_0^*(y)\psi_0$, and this implies for all $y \in Y$ the identity

$$S_Y P y = \psi_0^*(y) S_Y\psi_0 = \varepsilon_Y \psi_0^*(y)\psi_0 = \left(S_Y^*\psi_0^*\right)(y)\psi_0 = \psi_0^*\left(S_Y y\right)\psi_0 = P S_Y y \, ,$$

i.e., the operators P and S_Y commute.

In order to prove the remaining statement for Q, choose any $\varphi^* \in X^*$ with $\varphi^*(\varphi_0) \neq 0$. One can then write φ^* in the form $\varphi^* = \varphi_s^* + \varphi_a^*$, where $S_X^*\varphi_s^* = \varphi_s^*$ and $S_X^*\varphi_a^* = -\varphi_a^*$. Due to the inequality $\varphi^*(\varphi_0) \neq 0$, we can therefore find an element $\varphi_0^* \in X^*$ with $\varphi_0^*(\varphi_0) = 1$ and $S_X^*\varphi_0^* = \kappa\varphi_0^*$ for some $\kappa \in \{\pm 1\}$, as well as

$$\kappa = \kappa\varphi_0^*(\varphi_0) = S_X^*\varphi_0^*(\varphi_0) = \varphi_0^*(S_X\varphi_0) = \varphi_0^*(\varepsilon_X\varphi_0) = \varepsilon_X \, ,$$

i.e., we have $S_X^* \varphi_0^* = \varepsilon_X \varphi_0^*$. If we now define $Qx = \varphi_0^*(x)\varphi_0$ and $\tilde{X} = N(\varphi_0^*)$, then one finally obtains

$$S_X Q x = \varphi_0^*(x) S_X \varphi_0 = \varepsilon_X \varphi_0^*(x)\varphi_0 = S_X^* \varphi_0^*(x)\varphi_0 = \varphi_0^*(S_X x)\varphi_0 = Q S_X x \ ,$$

and the proof of the lemma is complete. □

Using these results, we can now show that equivariance also leads to the following symmetry properties in the method of Lyapunov-Schmidt.

Proposition 2.7 (Equivariant Lyapunov-Schmidt Reduction)**.** *Suppose that all the assumptions of Proposition 2.3 are satisfied, and that F is $\mathbb{Z}_2$-equivariant as in Definition 2.4. Finally, assume that $u_0 \in X_s$, and suppose that the projections P and Q are chosen as in Lemma 2.6(d). Then the following hold:*

(a) The nullspace $N(L)$ of $L = D_u F(\lambda_0, u_0)$ is invariant under S_X, and the range $R(L)$ is invariant under S_Y.

(b) The mapping W appearing in the the Lyapunov-Schmidt reduction in Proposition 2.3 is $\mathbb{Z}_2$-equivariant, i.e., we have

$$W(\lambda, S_X v) = S_X W(\lambda, v) \quad \text{for all} \quad \lambda \in \mathbb{R} \ \text{ and } \ v \in N(L) \ .$$

(c) The bifurcation function $b(\lambda, \alpha)$ satisfies

$$b(\lambda, \varepsilon_X \alpha) = \varepsilon_Y b(\lambda, \alpha) \quad \text{for all} \quad (\lambda, \alpha) \ \text{ close to } \ (\lambda_0, 0) \ ,$$

where ε_X and ε_Y encode the symmetry properties of φ_0 and ψ_0^*, respectively, as shown in Lemma 2.6.

Proof. The invariance of $N(L)$ and $R(L)$ follows immediately from (7) and $S_X u_0 = u_0$. To show (b), for arbitrary $\lambda \in \mathbb{R}$ and $v \in N(L)$ the equivariance of F, combined with the construction of W in the proof of Proposition 2.3 and Lemma 2.6(d) show

$$\begin{aligned}(I-P)F(\lambda, S_X v + S_X W(\lambda, v)) &= (I-P) S_Y F(\lambda, v + W(\lambda, v)) \\ &= S_Y \underbrace{(I-P)F(\lambda, v + W(\lambda, v))}_{= G(\lambda, v, W(\lambda, v))} \ = \ 0 \ ,\end{aligned}$$

which implies that $w = S_X W(\lambda, v)$ solves $G(\lambda, S_X v, w) = (I-P)F(\lambda, S_X v + w) = 0$. Due to the uniqueness property of W guaranteed by the implicit function theorem, this furnishes

$$S_X W(\lambda, v) = W(\lambda, S_X v) \ ,$$

i.e., the mapping W is $\mathbb{Z}_2$-equivariant. Finally, to show (c), for all $(\lambda, \alpha) \in \mathbb{R}^2$ close to $(\lambda_0, 0)$ we have

$$\begin{aligned}\varepsilon_Y b(\lambda, \alpha) &= \varepsilon_Y \psi_0^* P F(\lambda, v_0 + \alpha\varphi_0 + W(\lambda, v_0 + \alpha\varphi_0)) \\ &= S_Y^* \psi_0^* P F(\lambda, v_0 + \alpha\varphi_0 + W(\lambda, v_0 + \alpha\varphi_0)) \\ &= \psi_0^* S_Y P F(\lambda, v_0 + \alpha\varphi_0 + W(\lambda, v_0 + \alpha\varphi_0)) \\ &= \psi_0^* P F(\lambda, v_0 + \alpha S_X\varphi_0 + W(\lambda, v_0 + \alpha S_X\varphi_0)) \\ &= \psi_0^* P F(\lambda, v_0 + \alpha\varepsilon_X\varphi_0 + W(\lambda, v_0 + \alpha\varepsilon_X\varphi_0)) \\ &= b(\lambda, \varepsilon_X \alpha) \ ,\end{aligned}$$

where we have used the fact that $S_X v_0 = S_X Q u_0 = Q S_X u_0 = Q u_0 = v_0$. This completes the proof of the lemma. □

While in general it does not seem to be the case that ε_X and ε_Y have to be related, there are special situations when they have to coincide. One such situation is outlined in the following lemma, and it will be important for the application to the dibock copolymer model.

Our previous results give invariance conditions on symmetric spaces. However, there is no guarantee from these statements that a linear mapping preserves symmetry classes. The following result gives sufficient conditions on a linear mapping J under which we can guarantee that symmetric spaces are preserved rather than reversed. This will be critical in order to be able to state conditions for the occurence of a symmetry-breaking pitchfork bifurcation.

Lemma 2.8 (Forcing Sign Equality)**.** *Suppose that all the assumptions of Proposition 2.3 are satisfied, and that F is $\mathbb{Z}_2$-equivariant as in Definition 2.4. Assume that $u_0 \in X_s$, suppose that the projections P and Q are chosen as in Lemma 2.6(d), and let φ_0 and ψ_0^* define nullspace and range of the linearization $L = D_u F(\lambda_0, u_0)$ as before. Furthermore, suppose that there is a linear mapping $J : X \to Y$ which satisfies $JS_X = S_Y J$, as well as*

$$J\varphi_0 \notin R(L)\,, \qquad \text{or equivalently} \qquad \psi_0^* J\varphi_0 \neq 0\,.$$

Then the signs ε_X and ε_Y defined via $S_X\varphi_0 = \varepsilon_X\varphi_0$ and $S_Y^*\psi_0^* = \varepsilon_Y\psi_0^*$ satisfy $\varepsilon_X = \varepsilon_Y$, i.e., they necessarily coincide.

Proof. The assumptions immediately imply

$$\varepsilon_X \cdot \psi_0^* J\varphi_0 = \psi_0^* J\left(\varepsilon_X\varphi_0\right) = \psi_0^* JS_X\varphi_0 = \psi_0^* S_Y J\varphi_0 = S_Y^*\psi_0^* J\varphi_0 = \varepsilon_Y \cdot \psi_0^* J\varphi_0\,,$$

and dividing both sides by $\psi_0^* J\varphi_0 \neq 0$ furnishes the result. □

Notice that if Lemma 2.8 holds, then part (c) of Proposition 2.7 is particularly useful. In the nontrivial case, one has $\varepsilon_X = \varepsilon_Y = -1$, which immediately implies that the bifurcation equation $b(\lambda, \alpha) = 0$ is odd with respect to α — and therefore forces the existence of a trivial solution. This situation will correspond to symmetry-breaking bifurcations discussed further below.

2.2. **Saddle-node bifurcation points.** We now turn our attention to the first type of bifurcation considered in this paper — the saddle-node bifurcation. In generic systems, this is the only type of bifurcation point that can be observed. For this, assume that we have a solution (λ_0, u_0) of the problem (2), and that Assumption 2.2 holds. Then the condition

$$\psi_0^* D_\lambda F(\lambda_0, u_0) \neq 0 \tag{8}$$

is generically satisfied, and in this case one often refers to (λ_0, u_0) as a *simple saddle-node bifurcation point*, see for example [39]. In fact, the left-hand side of (8) is the first term in the Taylor expansion (5) of the bifurcation equation. In combination with the implicit function theorem this shows that under condition (8), the bifurcation equation $b(\lambda, \alpha) = 0$ can be solved for λ in a neighborhood of $(\lambda_0, 0)$. While this could lead to a situation where no bifurcation actually occurs, for example if the solution curve is monotone with respect to α, by assuming an additional generic condition one can guarantee a true saddle-node bifurcation point.

Proposition 2.9 (Existence of Saddle-Node Bifurcations)**.** *Suppose that Assumption 2.2 is satisfied and that (8) holds. If in addition the generic condition*

$$\psi_0^* D_{uu} F(\lambda_0, u_0)[\varphi_0, \varphi_0] \neq 0 \tag{9}$$

holds, then the nonlinear problem (2) undergoes a saddle-node bifurcation at (λ_0, u_0). *Furthermore, if* $\psi_0^* D_{uu} F(\lambda_0, u_0)[\varphi_0, \varphi_0] / \psi_0^* D_\lambda F(\lambda_0, u_0) > 0$, *then the bifurcating solutions exist for* $\lambda < \lambda_0$ *close to the bifurcation point, and if the ratio is negative for* $\lambda > \lambda_0$.

Proof. Proposition 2.3 shows that characterizing the solution set of (2) in a neighborhood of (λ_0, u_0) is equivalent to solving the bifurcation equation

$$b(\lambda_0 + \nu, \alpha) = 0 \tag{10}$$

in a neighborhood of $(0,0) \in \mathbb{R}^2$, where the Taylor expansion for b is given in (5). Due to (8) and the implicit function theorem there exists a smooth function $\nu = h(\alpha)$ which is defined in a neighborhood of 0 and whose graph contains all solutions of (10) in that neighborhood. In particular, we have $h(0) = 0$. Differentiating the identity $b(\lambda_0 + h(\alpha), \alpha) = 0$ twice with respect to α and then setting $\alpha = 0$ furnishes

$$\begin{aligned} D_\lambda b(\lambda_0, 0) h'(0) + D_\alpha b(\lambda_0, 0) &= 0 \,, \\ D_\lambda b(\lambda_0, 0) h''(0) + D_{\lambda\lambda} b(\lambda_0, 0) h'(0)^2 + 2 D_{\lambda\alpha} b(\lambda_0, 0) h'(0) + D_{\alpha\alpha} b(\lambda_0, 0) &= 0 \,. \end{aligned}$$

According to $D_\alpha b(\lambda_0, 0) = 0$ and $D_\lambda b(\lambda_0, 0) = \psi_0^* D_\lambda F(\lambda_0, u_0) \neq 0$ the first equation implies $h'(0) = 0$. Together with the second equation we finally obtain

$$h''(0) = -\frac{D_{\alpha\alpha} b(\lambda_0, 0)}{D_\lambda b(\lambda_0, 0)} = -\frac{\psi_0^* D_{uu} F(\lambda_0, u_0)[\varphi_0, \varphi_0]}{\psi_0^* D_\lambda F(\lambda_0, u_0)} \,,$$

which completes the proof of the lemma. □

While the above result provides generic conditions that guarantee a saddle-node bifurcation, we need to reformulate these to make them amenable to a rigorous computational approach which involves Newton's method. In other words, we need to derive a nonlinear system with an isolated zero which corresponds to the bifurcation point. For this, we follow the approach in [24] and consider a suitable extended system. More precisely, we supplement the nonlinear parameter-dependent equation (2) by another equation which forces the existence of an eigenfunction v of the appropriate Fréchet derivative, together with a normalizing condition on this eigenfunction. This leads to an extended system of the form

$$\begin{aligned} F(\lambda, u) &= 0 \,, \\ D_u F(\lambda, u)[v] &= 0 \,, \\ \ell(v) - 1 &= 0 \,, \end{aligned} \tag{11}$$

where $\ell \in X^*$ is a fixed element of the dual space of X. We abbreviate this system as

$$\mathcal{F}(\lambda, u, v) = (0, 0, 0) \,, \tag{12}$$

where

$$\mathcal{F} \;:\; \begin{cases} \mathbb{R} \times X \times X & \to & \mathbb{R} \times Y \times Y \\ (\lambda, u, v) & \mapsto & (\ell(v) - 1,\; F(\lambda, u),\; D_u F(\lambda, u)[v]) \end{cases} .$$

Then the following result is analogous to [24, 32]. Since in these two citations, the only operators acting on one Banach space are considered, we present the straightforward extension to mapping between different Banach spaces in detail.

Theorem 2.10 (Saddle-Node Bifurcations via Extended Systems)**.** *Suppose that Assumption 2.1 is satisfied. Then the following two statements hold.*

(a) *If the nonlinear operator F satisfies Assumption 2.2, as well as both conditions (8) and (9), and if $\ell \in X^*$ is any functional such that $\ell(\varphi_0) = 1$, then the Fréchet derivative $D_{(\lambda,u,v)}\mathcal{F}(\lambda_0, u_0, \varphi_0)$ is invertible, i.e., the solution $(\lambda_0, u_0, \varphi_0)$ of the extended system (11) is an isolated non-degenerate zero of the mapping $\mathcal{F}$.*

(b) *Conversely, if there exists an $\ell \in X^*$ and a $\varphi_0 \in X$ such that $\mathcal{F}(\lambda_0, u_0, \varphi_0) = (0, 0, 0)$, and if the Fréchet derivative $D_{(\lambda,u,v)}\mathcal{F}(\lambda_0, u_0, \varphi_0)$ is invertible, then the nonlinear operator F satisfies Assumption 2.2, as well as both conditions (8) and (9).*

Thus, the nonlinear problem (2) undergoes a saddle-node bifurcation at (λ_0, u_0) in the sense of Proposition 2.9, if and only if the triple $(\lambda_0, u_0, \varphi_0)$ is a non-degenerate zero of the nonlinear map $\mathcal{F}$ which defines the extended system (11).

Proof. (a) One can easily see that the Fréchet derivative of $\mathcal{F}$ is given by

$$D_{(\lambda,u,v)}\mathcal{F}(\lambda_0, u_0, \varphi_0)[\tilde\lambda, \tilde u, \tilde v] = \Big(\ell(\tilde v), \quad \tilde\lambda \cdot D_\lambda F(\lambda_0, u_0) + L\tilde u, \\ \tilde\lambda \cdot D_{\lambda u}F(\lambda_0, u_0)[\varphi_0] + D_{uu}F(\lambda_0, u_0)[\varphi_0, \tilde u] + L\tilde v\Big) \ ,$$

where we again use the abbreviation $L = D_u F(\lambda_0, u_0)$.

To begin with, we show that the Fréchet derivative is one-to-one. Assume that

$$D_{(\lambda,u,v)}\mathcal{F}(\lambda_0, u_0, \varphi_0)[\tilde\lambda, \tilde u, \tilde v] = (0, 0, 0).$$

We will now show that this implies $(\tilde\lambda, \tilde u, \tilde v) = (0, 0, 0)$. Applying ψ_0^* to the second component of the Fréchet derivative of $\mathcal{F}$, together with $R(L) = N(\psi_0^*)$, yields

$$0 \ = \ \tilde\lambda \cdot \psi_0^* D_\lambda F(\lambda_0, u_0) + \psi_0^* L\tilde u \ = \ \tilde\lambda \cdot \underbrace{\psi_0^* D_\lambda F(\lambda_0, u_0)}_{\neq 0} \ ,$$

and this in turn furnishes $\tilde\lambda = 0$. Substituting this identity into the second component one obtains $L\tilde u = 0$, i.e., there exists a constant $\gamma \in \mathbb{R}$ such that $\tilde u = \gamma\varphi_0$. Applying ψ_0^* to the third component of the Fréchet derivative of $\mathcal{F}$ then implies

$$0 \ = \ \psi_0^* D_{uu}F(\lambda_0, u_0)[\varphi_0, \tilde u] + \psi_0^* L\tilde v \ = \ \gamma \cdot \underbrace{\psi_0^* D_{uu}F(\lambda_0, u_0)[\varphi_0, \varphi_0]}_{\neq 0} \ ,$$

implying $\gamma = 0$, and $\tilde u = \gamma\varphi_0 = 0$. Now the third component reduces to $L\tilde v = 0$, which gives $\tilde v = \eta\varphi_0$. The first component then yields $0 = \ell(\tilde v) = \eta \cdot \ell(\varphi_0) = \eta$, i.e., we have $\tilde v = 0$. Thus the Fréchet derivative of $\mathcal{F}$ is one-to-one.

It remains to show that the Fréchet derivative is onto. Let $(\tau, y, z) \in \mathbb{R} \times Y \times Y$ be arbitrary. If we define $\tilde\lambda = \psi_0^* y / \psi_0^* D_\lambda F(\lambda_0, u_0)$, then there exists a unique $\tilde u \in \tilde X$ which satisfies $L\tilde u = y - \tilde\lambda D_\lambda F(\lambda_0, u_0)$, and for every $\gamma \in \mathbb{R}$ we have

$$\tilde\lambda \cdot D_\lambda F(\lambda_0, u_0) + L[\tilde u + \gamma\varphi_0] = y \ .$$

Now let $\gamma = \tilde\gamma$ denote the unique solution of the equation

$$\psi_0^* \Big(\tilde\lambda \cdot D_{\lambda u}F(\lambda_0, u_0)[\varphi_0] + D_{uu}F(\lambda_0, u_0)[\varphi_0, \tilde u + \gamma\varphi_0]\Big) = \psi_0^* z \ ,$$

which exists due to $\psi_0^* D_{uu}F(\lambda_0, u_0)[\varphi_0, \varphi_0] \neq 0$. Then there exists a unique $\tilde v \in \tilde X$ such that for all $\eta \in \mathbb{R}$ we have

$$\tilde\lambda \cdot D_{\lambda u}F(\lambda_0, u_0)[\varphi_0] + D_{uu}F(\lambda_0, u_0)[\varphi_0, \tilde u + \tilde\gamma\varphi_0] + L[\tilde v + \eta\varphi_0] = z \ .$$

If we finally define $\tilde{\eta} = \tau - \ell(\tilde{v})$, then one can easily verify that

$$D_{(\lambda,u,v)}\mathcal{F}(\lambda_0, u_0, \varphi_0)[\tilde{\lambda}, \tilde{u} + \tilde{\gamma}\varphi_0, \tilde{v} + \tilde{\eta}\varphi_0] \;=\; (\tau, y, z) \;,$$

and this completes the proof of (a).

(b) Now assume that there exists an $\ell \in X^*$ and a $\varphi_0 \in X$ such that $(\lambda_0, u_0, \varphi_0)$ is a non-degenerate zero of $\mathcal{F}$. According to the form of the third component of $\mathcal{F}$ we know that $\varphi_0 \in N(L)$. Assume there is another element $\varphi_1 \in N(L)$ which is linearly independent of φ_0. Then one can immediately verify that for all numbers $\alpha \in \mathbb{R}$ the linear combination

$$\varphi_\alpha = (1 - \alpha\ell(\varphi_1))\,\varphi_0 + \alpha\varphi_1 \qquad \text{satisfies} \qquad \ell(\varphi_\alpha) = 1 \;,$$

and is of course also in the kernel of L. This in turn implies that for all scalars $\alpha \in \mathbb{R}$ we have $\mathcal{F}(\lambda_0, u_0, (1 - \alpha\ell(\varphi_1))\varphi_0 + \alpha\varphi_1) = (0, 0, 0)$, i.e., the zero $(\lambda_0, u_0, \varphi_0)$ is not isolated and therefore the linearization of $\mathcal{F}$ at this point cannot be invertible. Thus, the operator $\mathcal{F}$ satisfies Assumption 2.2.

Now assume that (9) is not satisfied, i.e., we have $D_{uu}F(\lambda_0, u_0)[\varphi_0, \varphi_0] \in R(L)$. If we even have $D_{uu}F(\lambda_0, u_0)[\varphi_0, \varphi_0] = 0$, then one can see that $(\tilde{\lambda}, \tilde{u}, \tilde{v}) = (0, \varphi_0, 0)$ is a nontrivial element in the kernel of the linearization $D_{(\lambda,u,v)}\mathcal{F}(\lambda_0, u_0, \varphi_0)$, which violates its assumed invertibility. On the other hand, if $D_{uu}F(\lambda_0, u_0)[\varphi_0, \varphi_0] \neq 0$, then there exists a function $\hat{v} \notin N(L)$ such that $L\hat{v} = -D_{uu}F(\lambda_0, u_0)[\varphi_0, \varphi_0]$. In this case, one can verify that $(\tilde{\lambda}, \tilde{u}, \tilde{v}) = (0, 0, \hat{v} - \ell(\hat{v})\varphi_0)$ is a nontrivial element in the kernel of the linearization $D_{(\lambda,u,v)}\mathcal{F}(\lambda_0, u_0, \varphi_0)$, which again violates the assumed invertibility of the Fréchet derivative. This implies the validity of (9).

Finally, assume that (8) does not hold. This shows that $D_\lambda F(\lambda_0, u_0) \in R(L)$, and there exists a function $\hat{u}$ such that $L\hat{u} = -D_\lambda F(\lambda_0, u_0)$. Thus, for all $\alpha \in \mathbb{R}$ we have

$$D_\lambda F(\lambda_0, u_0) + L[\hat{u} + \alpha\varphi_0] = 0 \;.$$

Due to the already established validity of (9) and

$$\begin{aligned} D_{\lambda u}F(\lambda_0, u_0)[\varphi_0] + D_{uu}F(\lambda_0, u_0)[\varphi_0, \hat{u} + \alpha\varphi_0] = \\ D_{\lambda u}F(\lambda_0, u_0)[\varphi_0] + D_{uu}F(\lambda_0, u_0)[\varphi_0, \hat{u}] + \alpha \cdot D_{uu}F(\lambda_0, u_0)[\varphi_0, \varphi_0] \;, \end{aligned}$$

we can find a value $\hat{\alpha} \in \mathbb{R}$ such that

$$\psi_0^* \left(D_{\lambda u}F(\lambda_0, u_0)[\varphi_0] + D_{uu}F(\lambda_0, u_0)[\varphi_0, \hat{u} + \hat{\alpha}\varphi_0] \right) = 0 \;,$$

and therefore there exists a function $\hat{v} \in X$ such that

$$D_{\lambda u}F(\lambda_0, u_0)[\varphi_0] + D_{uu}F(\lambda_0, u_0)[\varphi_0, \hat{u} + \hat{\alpha}\varphi_0] + L\hat{v} = 0 \;.$$

This implies that the triple $(\tilde{\lambda}, \tilde{u}, \tilde{v}) = (1, \hat{u} + \hat{\alpha}\varphi_0, \hat{v} - \ell(\hat{v})\varphi_0)$ is contained in the kernel of the linearization $D_{(\lambda,u,v)}\mathcal{F}(\lambda_0, u_0, \varphi_0)$, violating the assumed non-degeneracy. Thus, (8) holds and the proof of the lemma is complete. □

The above lemma shows that generically, one can use standard path-following techniques to follow simple saddle-node bifurcation points as zeros of the system (12), as long as this system has an additional free parameter. This will be the case in our applications to the diblock copolymer model. Notice also that we do not have to separately establish the non-degeneracy conditions (8) and (9), as long as we can guarantee that the zero of the extended system is non-degenerate.

2.3. **Pitchfork bifurcation points forced by symmetry.** We now turn our attention to the case of pitchfork bifurcation points. Of course, such bifurcation points are non-generic in general systems. Nevertheless, our numerical path following results presented in the introduction clearly indicate that they do in fact occur in the diblock copolymer system. Unfortunately, however, at such pitchfork bifurcations the linearization of the extended system $\mathcal{F}$ defined in (12) in the previous section is no longer invertible — which prevents the use of Newton's method to locate them via a computer-assisted proof.

To remedy this problem we need to understand why these non-generic bifurcation points frequently do occur in partial differential equations. As it turns out, pitchfork bifurcations are usually forced through inherent symmetries. For the purposes of this paper, we assume that the symmetry occurs in the specific form introduced in Definition 2.4, i.e., via $\mathbb{Z}_2$-equivariance. It was shown in Proposition 2.7 that by choosing appropriate projections in the method of Lyapunov-Schmidt, equivariance propagates to the function W, and in some sense also to the bifurcation equation $b(\lambda, \alpha) = 0$ through the signs ε_X and ε_Y introduced in Lemma 2.6. If both of these signs are negative, we are in the situation of a symmetry-breaking bifurcation, and we have the following result.

Proposition 2.11 (Existence of Symmetry-Breaking Pitchfork Bifurcations)**.** *Suppose that Assumption 2.2 is satisfied and that F is $\mathbb{Z}_2$-equivariant as in Definition 2.4. Furthermore, assume that*

$$S_X u_0 = u_0 \,, \quad S_X \varphi_0 = -\varphi_0 \,, \qquad \text{as well as} \qquad S_Y^* \psi_0^* = -\psi_0^* \,, \tag{13}$$

that the projections P and Q are chosen as in Lemma 2.6(d), and that

$$\psi_0^* D_{\lambda u} F(\lambda_0, u_0)[\varphi_0] + \psi_0^* D_{uu} F(\lambda_0, u_0)[\varphi_0, \xi_0] \neq 0 \,, \tag{14}$$

where ξ_0 denotes the unique solution of the equation

$$D_u F(\lambda_0, u_0)[\xi_0] + (I - P) D_\lambda F(\lambda_0, u_0) = 0 \qquad \text{with} \qquad \xi_0 \in X_s \,. \tag{15}$$

Then the nonlinear problem (2) undergoes a pitchfork bifurcation at (λ_0, u_0). Locally at this point the solution set of (2) consists of a smooth solution curve parameterized by λ, together with a parabolic curve which is tangent to φ_0 at (λ_0, u_0). Consider the ratio

$$\varrho = \frac{\psi_0^* D_{uuu} F(\lambda_0, u_0)[\varphi_0, \varphi_0, \varphi_0] + 3\psi_0^* D_{uu} F(\lambda_0, u_0)[\varphi_0, \zeta_0]}{\psi_0^* D_{\lambda u} F(\lambda_0, u_0)[\varphi_0] + \psi_0^* D_{uu} F(\lambda_0, u_0)[\varphi_0, \xi_0]} \,,$$

where ξ_0 was defined in (15) and $\zeta_0 \in X_s$ is defined by

$$D_u F(\lambda_0, u_0)[\zeta_0] + (I - P) D_{uu} F(\lambda_0, u_0)[\varphi_0, \varphi_0] = 0 \,.$$

If the ratio ϱ is positive, then the solutions on the parabolic branch exist for $\lambda < \lambda_0$ close to the bifurcation point, if ϱ is negative then they exist for $\lambda > \lambda_0$. If $\varrho = 0$, either half of the branch could lie on either side of λ_0.

Proof. The assumptions of the proposition show that both Proposition 2.3 and Proposition 2.7 hold. In particular (13) implies that $\varepsilon_X = \varepsilon_Y = -1$. Thus, the left-hand side of the bifurcation equation $b(\lambda, \alpha) = 0$ satisfies

$$b(\lambda, -\alpha) = -b(\lambda, \alpha) \qquad \text{for all} \qquad (\lambda, \alpha) \;\text{ close to }\; (\lambda_0, 0) \,,$$

which immediately implies that $b(\lambda, 0) = 0$ as well as $D_{\alpha\alpha} b(\lambda, 0) = 0$ for all λ close to λ_0. Now define a function r in a neighborhood of $(\lambda_0, 0)$ by setting

$$r(\lambda, \alpha) = \begin{cases} \dfrac{b(\lambda, \alpha)}{\alpha} & \text{for} \quad \alpha \neq 0 \ , \\ \\ D_\alpha b(\lambda, 0) & \text{for} \quad \alpha = 0 \ . \end{cases}$$

Then in a neighborhood of $(\lambda_0, 0)$ the mapping r is smooth. Furthermore, it satisfies the identity $b(\lambda, \alpha) = \alpha \cdot r(\lambda, \alpha)$ — and this in turn shows that the bifurcation equation has the trivial solution branch $\alpha = 0$. From Proposition 2.3(a) this trivial branch gives rise to the smooth solution curve $\lambda \mapsto v_0 + W(\lambda, v_0)$ which is parameterized by λ and uses the projection $v_0 = Qu_0$. The mapping W is defined in Proposition 2.3, and Proposition 2.7(b) implies that W is equivariant.

In order to find the second solution branch, we need to solve the equation $r(\lambda, \alpha) = 0$. For this, notice that the definition of r and (5), together with the fact that $b(\lambda, 0) = 0$ for all λ close to λ_0 implies $D_{\lambda^k} b(\lambda_0, 0) = 0$ for all $k \geq 1$, lead to the expansion

$$r(\underbrace{\lambda_0 + \nu}_{=\lambda}, \alpha) = \nu \cdot D_{\lambda\alpha} b(\lambda_0, 0) + \frac{\nu^2}{2} \cdot D_{\lambda\lambda\alpha} b(\lambda_0, 0) + \frac{\alpha\nu}{2} \cdot D_{\lambda\alpha\alpha} b(\lambda_0, 0)$$

$$+ \ \frac{\alpha^2}{6} \cdot D_{\alpha\alpha\alpha} b(\lambda_0, 0) + R_r(\nu, \alpha) \ ,$$

with $R_r(\nu, \alpha) = O(\|(\nu, \alpha)\|^3)$. We clearly have $r(\lambda_0, 0) = D_\alpha b(\lambda_0, 0) = 0$, and (14) implies with Table 1 that $D_\lambda r(\lambda_0, 0) = D_{\lambda\alpha} b(\lambda_0, 0) \neq 0$. The implicit function theorem then yields a smooth function $\alpha \mapsto h(\alpha)$ which is defined near $\alpha = 0$, satisfies $h(0) = \lambda_0$, and such that in a neighborhood of $(0, 0)$ one has

$$r(\lambda, \alpha) = 0 \quad \text{ if and only if } \quad \lambda = h(\alpha) \ .$$

This establishes the second solution branch $\alpha \mapsto v_0 + \alpha\varphi_0 + W(h(\alpha), v_0 + \alpha\varphi_0)$.

In order to finish the proof, we only have to verify the tangency statement regarding the second solution branch, as well as its opening side. For this, one just has to differentiate the identity $r(h(\alpha), \alpha) = 0$ twice with respect to λ. One differentiation implies

$$D_\lambda r(h(\alpha), \alpha) h'(\alpha) + D_\alpha r(h(\alpha), \alpha) = 0 \ ,$$

which for $(\lambda, \alpha) = (\lambda_0, 0)$ gives $D_\lambda r(\lambda_0, 0) h'(0) + D_\alpha r(\lambda_0, 0) = 0$. Due to the inequality $D_\lambda r(\lambda_0, 0) \neq 0$, together with $D_\alpha r(\lambda_0, 0) = 0$, this implies $h'(0) = 0$. Computing the second derivative of $r(h(\alpha), \alpha) = 0$ with respect to α and then letting $\alpha = 0$ finally implies

$$D_\lambda r(\lambda_0, 0) h''(0) + D_{\alpha\alpha} r(\lambda_0, 0) = 0 \ ,$$

and therefore

$$h''(0) = -\frac{D_{\alpha\alpha} r(\lambda_0, 0)}{D_\lambda r(\lambda_0, 0)} = -\frac{D_{\alpha\alpha\alpha} b(\lambda_0, 0)}{3 D_{\lambda\alpha} b(\lambda_0, 0)} = -\frac{\varrho}{3} \ ,$$

where we also used Table 1. This completes the proof of the proposition. □

In order to rigorously determine the location of symmetry-breaking bifurcation points, we would like to consider an extended system similar to the one defined in (11) and (12). Unfortunately, if we were to consider this system as is, while the point $(\lambda_0, u_0, \varphi_0)$ would still be a zero, it would no longer be isolated and therefore preclude the use of any Newton-type method for its solution.

The prevalent role of symmetries in the formation of the pitchfork bifurcation allows for a simple adjustment. For this, we still consider the extended system as defined in (11) and (12). This time, however, one component of the map $\mathcal{F}_r$ induced by the system is restricted in domain and range to subspaces of X and Y, respectively. That is, we consider the restriction of the full system $\mathcal{F}$ given by

$$\mathcal{F}_r \;:\; \begin{cases} \mathbb{R}\times X_s\times X & \to & \mathbb{R}\times Y_s\times Y \\ (\lambda,u,v) & \mapsto & (\ell(v)-1,\; F(\lambda,u),\; D_uF(\lambda,u)[v]) \end{cases} \tag{16}$$

i.e., we restrict the argument u to the space of symmetric elements, and consider the image of the second component only in the symmetric subspace of Y. Notice that this restriction to Y_s in the image is justified by Lemma 2.5(a). Then the following result holds, which is in the spirit of a related result in [39], and extended to the case of different Banach spaces in domain and range.

Theorem 2.12 (Symmetry-Breaking Pitchfork Bifurcations via Extended Systems)**.** *Suppose that Assumption 2.1 is satisfied and that F is $\mathbb{Z}_2$-equivariant as in Definition 2.4. Then the following two statements hold.*

(a) Suppose that all assumptions of Proposition 2.11 are satisfied, and let $\ell\in X^*$ be such that $\ell(\varphi_0)=1$. Then the Fréchet derivative $D_{(\lambda,u,v)}\mathcal{F}_r(\lambda_0,u_0,\varphi_0)$ of the mapping in (16) is invertible, i.e., the solution $(\lambda_0,u_0,\varphi_0)\in\mathbb{R}\times X_s\times X$ of the extended system

$$\mathcal{F}_r(\lambda,u,\varphi)=(0,0,0) \tag{17}$$

is an isolated non-degenerate zero.

(b) Conversely, if there exists an $\ell\in X^*$ and a $\varphi_0\in X_a$ such that $(\lambda_0,u_0,\varphi_0)$ is a zero of the map $\mathcal{F}_r$, and if the Fréchet derivative $D_{(\lambda,u,v)}\mathcal{F}_r(\lambda_0,u_0,\varphi_0)$ is invertible, then the nonlinear operator F satisfies all assumptions of Proposition 2.11.

Thus, the problem (2) undergoes a symmetry-breaking pitchfork bifurcation at (λ_0,u_0) in the sense of Proposition 2.11, if and only if $(\lambda_0,u_0,\varphi_0)\in\mathbb{R}\times X_s\times X_a$ is a non-degenerate zero of (17).

Proof. (a) As before, the Fréchet derivative of $\mathcal{F}_r$ is given by

$$D_{(\lambda,u,v)}\mathcal{F}_r(\lambda_0,u_0,\varphi_0)[\tilde\lambda,\tilde u,\tilde v]=\Big(\ell(\tilde v),\quad \tilde\lambda\cdot D_\lambda F(\lambda_0,u_0)+L\tilde u,\\ \tilde\lambda\cdot D_{\lambda u}F(\lambda_0,u_0)[\varphi_0]+D_{uu}F(\lambda_0,u_0)[\varphi_0,\tilde u]+L\tilde v\Big)\;,$$

where we use the abbreviation $L=D_uF(\lambda_0,u_0)$. In the following, we assume that the projections P and Q have been chosen as in Lemma 2.6(d).

We begin by showing that the Fréchet derivative $D_{(\lambda,u,v)}\mathcal{F}_r(\lambda_0,u_0,\varphi_0)$ is one-to-one. For this, assume that $D_{(\lambda,u,v)}\mathcal{F}_r(\lambda_0,u_0,\varphi_0)[\tilde\lambda,\tilde u,\tilde v]=(0,0,0)$, and then show that this implies $(\tilde\lambda,\tilde u,\tilde v)=(0,0,0)$. To begin, suppose that $\tilde\lambda\neq 0$ — which will lead to a contradiction. Due to Lemmas 2.5(a) and 2.6(c) we have $D_\lambda F(\lambda_0,u_0)\in Y_s=L[X_s]\subset R(L)$, and together with $N(P)=R(L)$ this implies $PD_\lambda F(\lambda_0,u_0)=0$. Therefore the second component of the Fréchet derivative leads to

$$\tilde\lambda(I-P)D_\lambda F(\lambda_0,u_0)+L\tilde u=0\;,$$

which in turn implies $\xi_0=\tilde u/\tilde\lambda$, where ξ_0 is defined in (15). Plugging this into the third component of the Fréchet derivative yields

$$D_{\lambda u}F(\lambda_0,u_0)[\varphi_0]+D_{uu}F(\lambda_0,u_0)[\varphi_0,\xi_0]+L\tilde v/\tilde\lambda=0\;,$$

and applying ψ_0^*, together with $N(\psi_0^*) = R(L)$, results in

$$\psi_0^* D_{\lambda u} F(\lambda_0, u_0)[\varphi_0] + \psi_0^* D_{uu} F(\lambda_0, u_0)[\varphi_0, \xi_0] = 0 \, .$$

Since this last identity contradicts (14), we must have $\tilde{\lambda} = 0$. The second component of the Fréchet derivative then implies $L\tilde{u} = 0$, and therefore $\tilde{u} \in N(L) \cap X_s = \{0\}$. Now the third equation reduces to $L\tilde{v} = 0$, which gives $\tilde{v} \in N(L)$, i.e., we have $\tilde{v} = \eta\varphi_0$. The first component finally yields $0 = \ell(\tilde{v}) = \eta \cdot \ell(\varphi_0) = \eta$, i.e., one further obtains $\tilde{v} = 0$. In other words, the Fréchet derivative of $\mathcal{F}_r$ is one-to-one.

It remains to show that the Fréchet derivative is onto. Let $(\tau, y, z) \in \mathbb{R} \times Y_s \times Y$ be arbitrary. Since $y \in Y_s \subset R(L)$ and $N(L) \cap X_s = \{0\}$ there exists a unique element $\tilde{u} \in X_s$ such that

$$L\tilde{u} = y \, .$$

Now choose $\tilde{\lambda}$ via

$$\tilde{\lambda} = \frac{\psi_0^* z - \psi_0^* D_{uu} F(\lambda_0, u_0)[\varphi_0, \tilde{u}]}{\psi_0^* D_{\lambda u} F(\lambda_0, u_0)[\varphi_0] + \psi_0^* D_{uu} F(\lambda_0, u_0)[\varphi_0, \xi_0]} \, .$$

Then in combination with Lemma 2.5(b),(c) and $R(L) = N(\psi_0^*)$ one can show that

$$z - D_{uu} F(\lambda_0, u_0)[\varphi_0, \tilde{u}] - \tilde{\lambda} \cdot (D_{\lambda u} F(\lambda_0, u_0)[\varphi_0] + D_{uu} F(\lambda_0, u_0)[\varphi_0, \xi_0]) \in R(L) \, ,$$

and therefore there exists a $\tilde{v} \in X$ such that for all $\eta \in \mathbb{R}$ we have

$$\tilde{\lambda} \cdot D_{\lambda u} F(\lambda_0, u_0)[\varphi_0] + D_{uu} F(\lambda_0, u_0)[\varphi_0, \tilde{u} + \tilde{\lambda}\xi_0] + L[\tilde{v} + \eta\varphi_0] = z \, .$$

Furthermore, due to $L\tilde{u} = y$ we have

$$\tilde{\lambda} \cdot D_{\lambda} F(\lambda_0, u_0) + L[\tilde{u} + \tilde{\lambda}\xi_0] = -\tilde{\lambda} \cdot L\xi_0 + L[\tilde{u} + \tilde{\lambda}\xi_0] = L\tilde{u} = y \, .$$

If we finally define $\tilde{\eta} = \tau - \ell(\tilde{v})$, then employing the two previous identities one can easily verify that

$$D_{(\lambda,u,v)} \mathcal{F}_r(\lambda_0, u_0, \varphi_0)[\tilde{\lambda}, \tilde{u} + \tilde{\lambda}\xi_0, \tilde{v} + \tilde{\eta}\varphi_0] \;=\; (\tau, y, z) \;\; ,$$

and this completes the proof of (a).

(b) We now turn our attention to the proof of (b), and assume that there exists an $\ell \in X^*$ and a triple $(\lambda_0, u_0, \varphi_0) \in \mathbb{R} \times X_s \times X_a$ such that $\mathcal{F}_r(\lambda_0, u_0, \varphi_0) = (0, 0, 0)$, and that the Fréchet derivative of $\mathcal{F}_r$ at this point is invertible. Due to the specific form of the third component of $\mathcal{F}_r$ we have $\varphi_0 \in N(L)$. If there were another element $\varphi_1 \in N(L)$ which is linearly independent of φ_0, then one can immediately verify that for all $\alpha \in \mathbb{R}$ the linear combination $\varphi_\alpha = (1 - \alpha\ell(\varphi_1))\varphi_0 + \alpha\varphi_1$ satisfies $\ell(\varphi_\alpha) = 1$, and it is clearly also in the kernel of L. Thus, we have $\mathcal{F}_r(\lambda_0, u_0, (1 - \alpha\ell(\varphi_1))\varphi_0 + \alpha\varphi_1) = (0, 0, 0)$ for all $\alpha \in \mathbb{R}$, i.e., the zero $(\lambda_0, u_0, \varphi_0)$ is not isolated and therefore the linearization of $\mathcal{F}_r$ at this point cannot be invertible. Thus, the operator $\mathcal{F}_r$ satisfies Assumption 2.2.

From our assumptions, we already know that $S_X u_0 = u_0$, that $S_X \varphi_0 = -\varphi_0$, and we can choose the projections P and Q as in Lemma 2.6(d). In addition, we have $S_Y^* \psi_0^* = \varepsilon_Y \psi_0^*$ for some as of yet unknown sign $\varepsilon_Y \in \{\pm 1\}$. Finally, since the projection $I - P$ maps X_s into $Y_s \cap R(L)$ and since $N(L) \cap X_s = \{0\}$, Lemma 2.5(a) shows that there exists a unique $\xi_0 \in X_s$ which solves (15).

In order to establish $\varepsilon_Y = -1$, we first show that in fact $L[X_s] = Y_s$. For this, let $z_s \in Y_s$ be arbitrary. Since the derivative $D_{(\lambda,u,v)} \mathcal{F}_r(\lambda_0, u_0, \varphi_0)$ is invertible, there exists $(\tilde{\lambda}, \tilde{u}, \tilde{v}) \in \mathbb{R} \times X_s \times X$ with $D_{(\lambda,u,v)} \mathcal{F}_r(\lambda_0, u_0, \varphi_0)[\tilde{\lambda}, \tilde{u}, \tilde{v}] = (0, 0, z_s)$, which in turn implies the identity

$$\tilde{\lambda} \cdot D_{\lambda u} F(\lambda_0, u_0)[\varphi_0] + D_{uu} F(\lambda_0, u_0)[\varphi_0, \tilde{u}] + L\tilde{v} = z_s \, .$$

If we now decompose $\tilde{v} \in X$ as $\tilde{v} = \tilde{v}_s + \tilde{v}_a \in X_s \oplus X_a$, then Lemma 2.5(b),(c) implies

$$\underbrace{L\tilde{v}_s}_{\in Y_s} + \underbrace{L\tilde{v}_a}_{\in Y_a} = \underbrace{z_s}_{\in Y_s} - \underbrace{\Big(\tilde{\lambda} \cdot D_{\lambda u}F(\lambda_0, u_0)[\varphi_0] + D_{uu}F(\lambda_0, u_0)[\varphi_0, \tilde{u}]\Big)}_{\in Y_a} ,$$

and together with $Y = Y_s \oplus Y_a$ this leads to $L\tilde{v}_s = z_s$, i.e., we have $L[X_s] = Y_s$. In view of Lemma 2.6(c), one therefore has to have $\varepsilon_Y = -1$, i.e., the equalities in (13) hold.

It remains to show that (14) is satisfied. For this, let $z \in Y \setminus R(L)$ be arbitrary. Then the assumptions of (b) imply that there exists a $(\tilde{\lambda}, \tilde{u}, \tilde{v}) \in \mathbb{R} \times X_s \times X$ such that

$$D_{(\lambda,u,v)}\mathcal{F}_r(\lambda_0, u_0, \varphi_0)[\tilde{\lambda}, \tilde{u}, \tilde{v}] = (0, 0, z) . \tag{18}$$

Assume for the moment that we have in fact $\tilde{\lambda} = 0$. Then the equation for the second components of (18) implies $L\tilde{u} = 0$, which in turn gives $\tilde{u} \in N(L) \cap X_s = \{0\}$. But in this case the last component of (18) reduces to $L\tilde{v} = z \notin R(L)$, which is impossible. Thus, we necessarily have to have $\tilde{\lambda} \neq 0$, and the second component in (18) implies in combination with $D_\lambda F(\lambda_0, u_0) \in Y_s \subset R(L) = N(P)$ the identity

$$(I - P)D_\lambda F(\lambda_0, u_0) + L[\tilde{u}/\tilde{\lambda}] = D_\lambda F(\lambda_0, u_0) + L[\tilde{u}/\tilde{\lambda}] = 0 ,$$

i.e., according to (15) one obtains $\tilde{u} = \tilde{\lambda}\xi_0$. Substituting this expression into the last component of (18) finally yields

$$\tilde{\lambda}D_{\lambda u}F(\lambda_0, u_0)[\varphi_0] + D_{uu}F(\lambda_0, u_0)[\varphi_0, \tilde{\lambda}\xi_0] + L\tilde{v} = z ,$$

and applying ψ_0^* to both sides leads to

$$\tilde{\lambda} \cdot (\psi_0^* D_{\lambda u}F(\lambda_0, u_0)[\varphi_0] + \psi_0^* D_{uu}F(\lambda_0, u_0)[\varphi_0, \xi_0]) = \psi_0^* z \neq 0 ,$$

due to $\psi_0^* L\tilde{v} = 0$ and $z \notin R(L)$. This establishes (14), and therefore all assumptions of Proposition 2.11 are satisfied. This completes the proof of the theorem. □

Remark 2.13 (Alternative Expressions for ξ_0 and ζ_0)**.** The proof of the above theorem shows that the functions $\xi_0 \in X_s$ and $\zeta_0 \in X_s$ defined in Proposition 2.11 can equivalently be defined as solutions of the two identities

$$D_u F(\lambda_0, u_0)[\xi_0] = -D_\lambda F(\lambda_0, u_0) ,$$

$$D_u F(\lambda_0, u_0)[\zeta_0] = -D_{uu}F(\lambda_0, u_0)[\varphi_0, \varphi_0] ,$$

which no longer include the projection P.

As in the previous subsection, the above theorem shows that generically, one can use standard Newton-type techniques to determine symmetry-breaking pitchfork bifurcation points as zeros of the system (17). This time, however, the system is restricted to symmetry subspaces, and this will in fact lead to significant reductions in dimensions later on.

To close this section, let us briefly contrast the reduced system (17) to the one considered in [39]. As we mentioned earlier, this reference is concerned with a numerical method for computing the location of symmetry-breaking pitchfork bifurcations, and it employs the even further restricted system $\mathcal{F}_{rr}(\lambda, u, v) = (0, 0, 0)$, where

$$\mathcal{F}_{rr} \;:\; \left\{ \begin{array}{rcl} \mathbb{R} \times X_s \times X_a & \to & \mathbb{R} \times Y_s \times Y_a \\ (\lambda, u, v) & \mapsto & (\ell(v) - 1,\ F(\lambda, u),\ D_u F(\lambda, u)[v]) \end{array} \right. \tag{19}$$

i.e., they restrict the argument u to the space of symmetric elements, and the argument v to the space of antisymmetric elements. From a purely computational point of view, this system leads to a reliable method. We would like to point out, however, that it cannot easily be used in a computer-assisted proof setting. As the following example shows, even if the system $\mathcal{F}_{rr}(\lambda, u, v) = (0, 0, 0)$ has an isolated zero, this does not guarantee the existence of a symmetry-breaking pitchfork bifurcation as in Proposition 2.11. The reason for this surprising behavior lies in the fact that even for an isolated zero of this further reduced system, the Fréchet derivative $D_u F(\lambda_0, u_0)$ does not necessarily have a one-dimensional kernel; it could be higher-dimensional. While this precludes a computer-assisted proof, it does work in a purely numerical setting, since in this setting the kernel is almost-surely one-dimensional.

Example 2.14 (Degenerate Symmetry-Breaking Bifurcations)**.** In this example we show that even if the reduced system $\mathcal{F}_{rr}(\lambda, u, v) = (0, 0, 0)$, with $\mathcal{F}_{rr}$ as in (19), has an isolated zero, this does not mean that the Fréchet derivative of the underlying map F has a one-dimensional kernel. To see this, consider the class of functions suggested in [39], which are of the form

$$F(\lambda, (x_1, x_2)) = (f(\lambda, x_1), f(\lambda, x_2)) \,,$$

where $f : \mathbb{R}^2 \to \mathbb{R}$ will be specified later on. If we let $X = Y = \mathbb{R}^2$, then one can easily see that the mapping $F : \mathbb{R} \times X \to Y$ is $\mathbb{Z}_2$-equivariant with respect to the symmetries

$$S_X = S_Y = \begin{pmatrix} 0 & 1 \\ 1 & 0 \end{pmatrix} \,,$$

and the symmetric and antisymmetric subspaces are given by

$$X_s = \{(x_1, x_2) : x_1 = x_2\} \quad \text{and} \quad X_a = \{(x_1, x_2) : x_1 = -x_2\} \,.$$

Based on the form of F, if there is a curve $(\lambda, x(\lambda))$ such that $f(\lambda, x(\lambda)) = 0$ holds, then we automatically have $F(\lambda, x(\lambda), x(\lambda)) = (0, 0)$. Consider now the specific function

$$f(\lambda, y) = y - \frac{\lambda}{1 - y^2} \,.$$

Then one can easily see that $f(\lambda, y) = 0$ whenever we have $\lambda = y - y^3$. Moreover, if we define $\lambda_\pm = \pm 2/(3\sqrt{3})$ and $x_\pm = \pm 1/\sqrt{3}$, then

$$\frac{\partial f}{\partial y}(\lambda_\pm, x_\pm) = 0 \,,$$

which in turn implies

$$D_{(x_1,x_2)} F(\lambda_\pm, x_\pm, x_\pm) = \begin{pmatrix} 0 & 0 \\ 0 & 0 \end{pmatrix} \,.$$

Thus, the Fréchet derivative $D_{(x_1,x_2)} F(\lambda_\pm, x_\pm, x_\pm)$ has a two-dimensional kernel on X, and a one-dimensional kernel on X_a. One can show that despite the fact that $(\lambda_\pm, x_\pm, x_\pm)$ are isolated solutions of the system $\mathcal{F}_{rr}(\lambda, u, v) = (0, 0, 0)$, the bifurcation at these two points is not a pitchfork bifurcation in the sense of Proposition 2.11. Rather, at each point we have a degenerate bifurcation point. See also Figure 2. The same type of degenerate bifurcation occurs for the coupled cell reaction model with an Arrhenius reaction rate term in Example 4.1 of [39] with $\varepsilon = 0$. These simple examples illustrate the general problem that we cannot determine the kernel of the linearization by only looking at the antisymmetric part of the space.

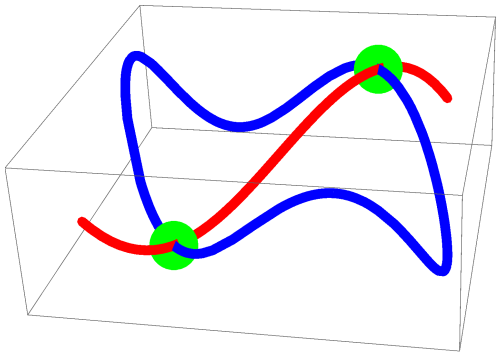

FIGURE 2. Two degenerate symmetry-breaking bifurcations as described in Example 2.14.

2.4. **Application to the diblock copolymer equation.** In this section we demonstrate how the diblock copolymer model (1) fits into the framework described above. For more details we refer the reader to [17]. Rather than studying the model in the form described in the introduction, we apply the transformation $u \mapsto \mu + u$ so that in the following we always consider the mass constraint zero and have incorporated μ into the equation. After this transformation, finding equilibrium solutions of the evolution equation is equivalent to solving the nonlinear operator equation

$$F(\lambda, u) \;=\; -\left(u_{xx} + \lambda f(\mu + u)\right)_{xx} - \lambda\sigma u \;=\; 0\,, \tag{20}$$

where F is a parameter-dependent operator $F : \mathbb{R} \times X \to Y$ on the Hölder-type spaces

$$X = \Big\{ u \in C^{4,\varrho}[0,1] \;:\; \int_0^1 u(x)\,dx = 0 \;\text{ and } \\ u_x(0) = u_{xxx}(0) = u_x(1) = u_{xxx}(1) = 0 \Big\}\,, \tag{21}$$

$$Y = \Big\{ u \in C^{0,\varrho}[0,1] \;:\; \int_0^1 u(x)\,dx = 0 \Big\}\,,$$

and with nonlinearity $f(u) = u - u^3$. In order to keep our notation uniform throughout the section, we only emphasize the parameter λ in the definition of F, since this is our primary bifurcation parameter. However, the secondary parameter σ will prove to be essential in order to find location curves of bifurcation points in the diblock copolymer model. Notice also that for every choice of the parameters λ, σ, and μ the constant function $u \equiv 0$ satisfies (20). This solution is referred to as the *trivial solution*.

The bifurcation diagram of (20) in a neighborhood of the trivial solution has been completely described in [17] using a standard Lyapunov-Schmidt approach. In order to describe these results, note that the eigenvalues and eigenfunctions of the negative Laplacian $-\Delta$ on the one-dimensional domain $\Omega = (0,1)$ and subject to homogeneous Neumann boundary conditions, are given by

$$\kappa_k = k^2\pi^2 \quad \text{and} \quad \varphi_k(x) = \sqrt{2}\cos k\pi x \quad \text{for} \quad k \in \mathbb{N}\,. \tag{22}$$

Since the space X contains a mass constraint, the constant eigenfunction with eigenvalue zero will play no role in the following and has therefore been omitted. Using this notation, it was shown in [17] that the bifurcation points from the trivial solution of (20) are given by

$$\lambda(k,\sigma,\mu) = \frac{\kappa_k^2}{f'(\mu)\cdot\kappa_k - \sigma}\ , \tag{23}$$

where $\sigma \geq 0$. Since we are only interested in bifurcation points at positive λ-values, the indices k have to satisfy $\kappa_k > \sigma/f'(\mu)$, and one needs to assume that $f'(\mu) > 0$, i.e. the total mass μ has to be in the spinodal region.

It was shown in [17], and briefly described in the introduction, that most of the solution branches of (20) which bifurcate from the trivial solution undergo a variety of secondary bifurcations. Studying these secondary bifurcation points using rigorous computational techniques is the main subject of this paper. For this, we need to first show that the nonlinear mapping F defined above satisfies all the conditions of the abstract results described so far. This will be accomplished in the following proposition.

Proposition 2.15. *Consider the nonlinear operator F defined in the diblock copolymer equilibrium equation (20), and let the Banach spaces X and Y be defined as in (21). Furthermore, assume that $(\lambda_0, u_0) \in \mathbb{R}^+ \times X$ is arbitrary, and that $\sigma = \sigma_0 > 0$ and $\mu = \mu_0 \in \mathbb{R}$ are fixed. Then the following hold.*

(a) The Fréchet derivative $L = D_u F(\lambda_0, u_0) \in \mathcal{L}(X,Y)$ is a Fredholm operator of index zero.

(b) The kernel $N(L)$ is spanned by linearly independent solutions $\varphi_0, \ldots, \varphi_{n-1}$ of the linear elliptic problem

$$Lv = -\left(v_{xx} + \lambda_0 f'(\mu_0 + u_0)v\right)_{xx} - \lambda_0\sigma_0 v = 0 \quad \text{with} \quad v \in X\ ,$$

i.e., the functions φ_k solve this linear differential equation subject to the zero mass constraint and Neumann boundary conditions as in (1).

(c) If $\psi_0, \ldots, \psi_{n-1} \in C^{4,\varrho}[0,1]$ denote n linearly independent solutions of the adjoint problem

$$L^* w = -w_{xxxx} - \lambda_0 f'(\mu_0 + u_0) w_{xx} - \lambda_0\sigma_0 w = 0\ ,$$

subject to the Neumann conditions $w_x(0) = w_{xxx}(0) = w_x(1) = w_{xxx}(1) = 0$, but without imposing any integral constraint, then the range of L is characterized by

$$R(L) = \left\{ w \in Y \ : \ \int_0^1 \psi_k(x) w(x)\, dx = 0 \quad \text{for all} \quad k = 0, \ldots, n-1 \right\}\ .$$

Proof. Rather than considering X and Y directly, we first consider the standard Hölder spaces without mass constraint given by

$$\mathcal{X} = \left\{ u \in C^{4,\varrho}[0,1] \ : \ u_x(0) = u_{xxx}(0) = u_x(1) = u_{xxx}(1) = 0 \right\},$$

$$\mathcal{Y} = \left\{ u \in C^{0,\varrho}[0,1] \right\}\ .$$

Then $F : \mathbb{R}\times\mathcal{X} \to \mathcal{Y}$ is a smooth nonlinear operator. In fact, standard elliptic theory shows that in this setting, the operator F is a Fredholm operator of index zero: For any choice of $\lambda_0, \sigma_0, \mu_0 \in \mathbb{R}$ and any $u_0 \in \mathcal{X}$ the linearization $L = D_u F(\lambda_0, u_0)$ is an elliptic operator with principal term $-v_{xxxx}$. The latter operator is Fredholm with index zero, since in the associated Sobolev setting it is in fact self-adjoint. Since

the additional terms in L are of lower differentiation order, they are a compact perturbation, and (a) follows for L, but with $\mathcal{X}$ and $\mathcal{Y}$ replacing X and Y. For more details we refer the reader to [41, pp. 259ff].

We now turn our attention to the operator F restricted to the spaces X and Y which impose the zero mass constraint. To begin with, it is easy to see that for any $\lambda_0 \in \mathbb{R}$ and $u_0 \in X$ one has $F(\lambda_0, u_0) \in Y$, i.e., considering F as an operator from $\mathbb{R} \times X$ into Y is well-defined. Similarly, we have $L(X) \subset Y$. But even more is true. If $v \in \mathcal{X}$ is arbitrary, then

$$\int_0^1 Lv(x)\,dx = -\lambda_0\sigma_0 \cdot \int_0^1 v(x)\,dx\ ,$$

due to the imposed boundary conditions and integration by parts. The latter identity, together with our assumptions $\lambda_0 \neq 0$ and $\sigma_0 \neq 0$, furnishes:

$$\text{For every}\ \ v \in \mathcal{X} \setminus X\ \ \text{we have}\ \ Lv \in \mathcal{Y} \setminus Y\ . \tag{24}$$

This identity will prove to be essential below. Now let

$$N\left(L|_{\mathcal{X}}\right) = \operatorname{span}[\varphi_0, \ldots, \varphi_{n-1}] \subset \mathcal{X}$$

denote the nullspace of $L|_{\mathcal{X}}$ considered as operator between $\mathcal{X}$ and $\mathcal{Y}$, and let

$$N\left(L^*|_{\mathcal{X}}\right) = \operatorname{span}[\psi_0, \ldots, \psi_{n-1}] \subset \mathcal{X}$$

denote the nullspace of $L^*|_{\mathcal{X}}$ considered as operator between $\mathcal{X}$ and $\mathcal{Y}$. Due to our above discussion, both nullspaces have to have the same finite dimension n. Furthermore, property (24) immediately shows that

$$N\left(L|_{\mathcal{X}}\right) \subset X\ , \quad \text{i.e., we have} \quad \dim N\left(L|_X\right) = \dim N\left(L|_{\mathcal{X}}\right) = n\ .$$

We now turn our attention to the characterization of the range of L. According to the closed range theorem, the operator $L|_{\mathcal{X}} : \mathcal{X} \to \mathcal{Y}$ satisfies

$$R\left(L|_{\mathcal{X}}\right) = \left\{ w \in \mathcal{Y}\ :\ \int_0^1 \psi_k(x) w(x)\,dx = 0 \quad \text{for all} \quad k = 0, \ldots, n-1 \right\}\ . \tag{25}$$

It is clear from the form of the adjoint operator $L^*|_{\mathcal{X}}$ that the functions ψ_k are in general not in the space X. Thus, choose $\alpha_0, \ldots, \alpha_{n-1} \in \mathbb{R}$ and $\bar{\psi}_0, \ldots, \bar{\psi}_{n-1} \in X$ such that $\psi_k = \alpha_k + \bar{\psi}_k$ for all $k = 0, \ldots, n-1$. We claim that the functions $\bar{\psi}_0, \ldots, \bar{\psi}_{n-1} \in X$ are linearly independent. For this, assume that $\gamma_0, \ldots, \gamma_{n-1} \in \mathbb{R}$ are such that

$$0 = \sum_{k=0}^{n-1} \gamma_k \cdot \bar{\psi}_k = \sum_{k=0}^{n-1} \gamma_k \cdot (\psi_k - \alpha_k) = \sum_{k=0}^{n-1} \gamma_k \psi_k - \sum_{k=0}^{n-1} \gamma_k \alpha_k\ .$$

Applying $L^*|_{\mathcal{X}}$ on both sides, together with the fact that every constant function is an eigenfunction of $L^*|_{\mathcal{X}}$ with eigenvalue $-\lambda_0\sigma_0$, then furnishes

$$0 = \sum_{k=0}^{n-1} \gamma_k \underbrace{L^*\psi_k}_{=0} - L^* \underbrace{\sum_{k=0}^{n-1} \gamma_k \alpha_k}_{=\text{const}} = \lambda_0\sigma_0 \cdot \sum_{k=0}^{n-1} \gamma_k \alpha_k\ ,$$

which due to $\lambda_0\sigma_0 \neq 0$ finally implies

$$\sum_{k=0}^{n-1} \gamma_k \psi_k = \sum_{k=0}^{n-1} \gamma_k \alpha_k = 0\ .$$

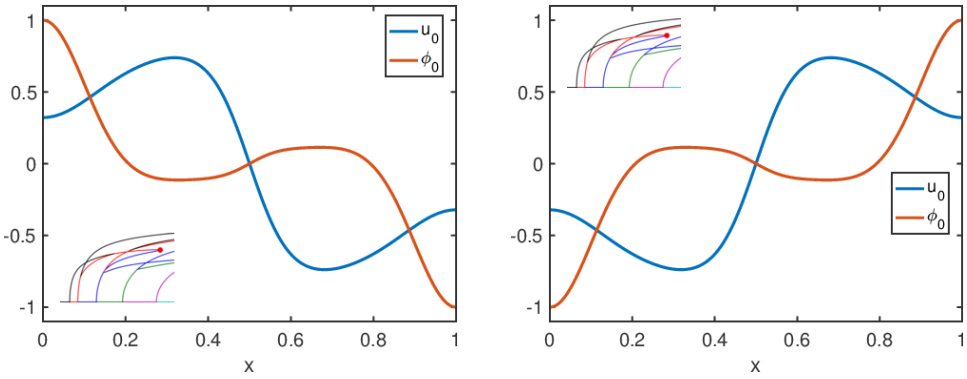

FIGURE 3. Equilibrium solutions u_0 (in blue) of the diblock copolymer equation for $\sigma_0 = 6$, together with their associated kernel functions φ_0 (in orange). These two distinct stationary solutions are both saddle-node bifurcation points at the same parameter value $\lambda_0 \approx 262.9$ and the same L^2-norm close to 0.562. In fact, the entire non-trivial portion of the bifurcation diagram is multiply covered. These equilibria are rigorously proved in Theorem 3.7.

The assumed linear independence of $\psi_0, \dots, \psi_{n-1}$ then yields $\gamma_1 = \dots = \gamma_{n-1} = 0$, and therefore also the reduced functions $\bar{\psi}_0, \dots, \bar{\psi}_{n-1}$ are linearly independent.

After these preparations we can now easily complete the proof of Proposition 2.15. With the help of (24) one can show that

$$R\,(L|_X) = R\,(L|_{\mathcal{X}}) \cap Y\ ,$$

and this furnishes with (25) the identity

$$R\,(L|_X) = \left\{ w \in Y \ : \ \int_0^1 \psi_k(x) w(x)\,dx = 0 \quad \text{for all} \quad k = 0, \dots, n-1 \right\}$$

$$= \left\{ w \in Y \ : \ \int_0^1 \bar{\psi}_k(x) w(x)\,dx = 0 \quad \text{for all} \quad k = 0, \dots, n-1 \right\}\ .$$

Since $\bar{\psi}_0, \dots, \bar{\psi}_{n-1}$ are linearly independent in Y, the range $R(L|_X) \subset Y$ therefore has codimension n in Y, which equals the dimension of the nullspace $N(L|_X) \subset X$. This completes the proof. □

The above proposition shows that despite imposing the mass constraint both in the domain and in the range of the nonlinear operator, we retain the crucial Fredholm property. We would also like to stress again the point that the solutions $\psi_0, \dots, \psi_{n-1}$ of the adjoint problem, which are used to characterize the range of L, do not in general satisfy the zero mass constraint. Finally, if in Proposition 2.15 the kernel is one-dimensional, and if we define a functional $\psi_0^* \in Y^*$ via

$$\psi_0^*(w) = \int_0^1 \psi_0(x) w(x)\,dx\ ,$$

then one can readily see that $R(L) = N(\psi_0^*)$, i.e., we are exactly in the situation of Assumption 2.2.

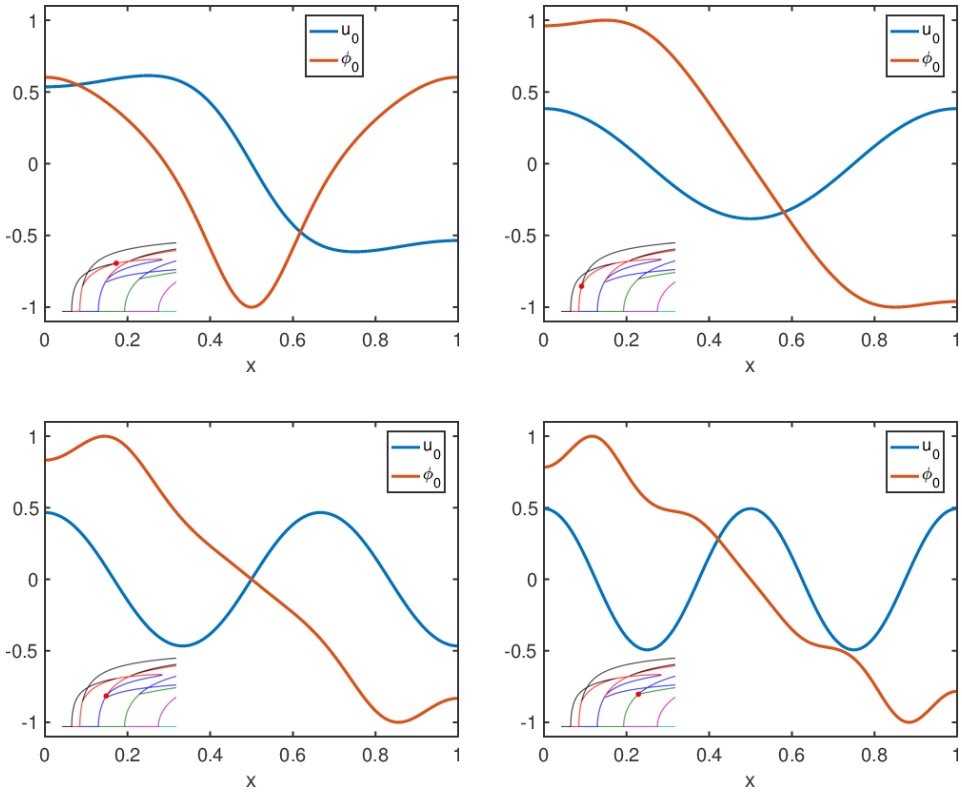

FIGURE 4. Equilibrium solutions u_0 (in blue) and associated kernel functions φ_0 (in orange) of the diblock copolymer equation for $\sigma_0 = 6$, with $\lambda_0 \approx 142.1, 53.6, 203.1$ for top left, top right, and bottom right, respectively. All four solutions are pitchfork bifurcation points. They are the first bifurcation points on the first four branches bifurcating from the trivial solution in the right image sof Figure 1. Note that as in Figure 3, the bifurcation diagram is a double cover; corresponding to each of these four solutions, there is another solution at the same point in the bifurcation diagram. See also Theorems 3.13, 3.14, and 3.15.

Proposition 2.15 enables us to apply the general results of the previous sections to the diblock copolymer model. For example, we can use the nonlinear system (11) to determine saddle-node bifurcation points via a standard Newton iteration, see also Theorem 2.10. Examples of such saddle-node bifurcation points are shown in Figure 3.

Similarly, we can use symmetry methods to establish the location of symmetry-breaking pitchfork bifurcation points via the solution of the extended system (16) using Newton's method, see also Theorem 2.12. For this, of course, we need to specify suitable symmetry operations. Consider for example the symmetry operators S_X and S_Y defined via

$$(S_2 u)(x) = u(1-x) \quad \text{for} \quad u \in X \quad \text{or} \quad u \in Y \,,$$

i.e., via the same formula in both X and Y. Since $X \subset Y$ is embedded via the identity map, we can apply Lemma 2.8 with $J = I$. This implies that if $\varphi_0 \notin R(L)$, then the signs ε_X and ε_Y in Lemma 2.6 necessarily have to agree. In the right column of Figure 4, two equilibrium solutions of the diblock copolymer model are depicted in orange, along with the kernel functions of the Fréchet derivative $D_u F(\lambda_0, u_0)$, which are shown in blue. These solutions are symmetry-breaking pitchfork bifurcation points which lie on the second and fourth bifurcation branches from the trivial solution curve shown in the right image of Figure 1. The equilibria are symmetric elements with respect to the above symmetry S, and the associated kernel functions are antisymmetric. Thus these solutions satisfy the symmetry conditions needed for a symmetry-breaking pitchfork bifurcation, and in both of these cases, Proposition 2.15 will enable us to use Theorem 2.12 to rigorously prove their existence.

But what about the pitchfork bifurcation points on the first, third and fifth branches shown in the right image of Figure 1? In these cases, the solutions on the branch are no longer symmetric elements. If instead we define a new symmetry operator via

$$(S_1 u)(x) = -u(1-x) \quad \text{for} \quad u \in X \quad \text{or} \quad u \in Y \,,$$

then the pitchfork bifurcation points are again symmetric elements. The corresponding solutions for the first and third branch are shown in the left column of Figure 4 along with their associated kernel functions. Since the kernel function in the upper left panel is antisymmetric with respect to this new symmetry, this is a symmetry-breaking bifurcation point which can be treated using Theorem 2.12, but with respect to the new symmetry. In contrast, the solution and kernel function of the third branch solution in the lower left panel are both symmetric with respect to the new symmetry. This implies that our symmetry-breaking pitchfork bifurcation result no longer applies. In fact, this bifurcation is not a $\mathbb{Z}_2$-symmetry-breaking bifurcation, but rather a symmetry-breaking bifurcation with a different equivariance group. Thus a different approach is needed to treat this bifurcation, and we will address this in a future paper.

3. **Rigorous verification of bifurcations.** As already mentioned in Section 2.4, Proposition 2.15 enables us to study saddle-node and pitchfork bifurcation points via Theorem 2.10 and Theorem 2.12, respectively. In particular, by Theorem 2.10, proving existence of a non-degenerate isolated zero of (12) implies the existence of a saddle-node bifurcation, and by Theorem 2.12, proving existence of a non-degenerate isolated zero of (17) implies the existence of a pitchfork bifurcation.

In this section, we use the tools of rigorous computing (e.g. see [33]) to verify existence of bifurcations in the diblock copolymer equation. In order to do so, we begin by presenting the equivalent of (11) in the space of Fourier coefficients. We note that the reformulation of a function space problem in terms of an infinite series is standard as both a numerical and analytical technique, but it also has a long history as a method of computer-assisted proof, such as for example in Lanford's proof of the Feigenbaum conjectures [18]. Note that while our general results in previous sections establish conclusions in the the more general case of Hölder continuity, since we are considering the space of Fourier coefficients, our results in this section have much more additional regularity than just Hölder continuity. Namely, we are able to rigorously establish real analytic bifurcating solutions.

Consider the steady states diblock copolymer equation (20) with $f(u) = u - u^3$. Our results apply for all values of μ, but in order for the mass constraint to allow

for both symmetric and asymmetric solutions, in our numerics, we fix $\mu = 0$. That is

$$F(\lambda, u) = -\left(u_{xx} + \lambda(u - u^3)\right)_{xx} - \lambda\sigma u = 0.$$

Plugging the cosine Fourier expansion

$$u(x) = \sum_{k\in\mathbb{Z}} a_k e^{ik\pi x} = 2\sum_{k\geq 1} a_k \cos(k\pi x),\ (a_k \in \mathbb{R},\ a_{-k} = a_k,\ a_0 = 0) \tag{26}$$

in $F(\lambda, u) = 0$ leads to $\sum_{k\in\mathbb{Z}} g_k e^{ik\pi x} = 0$, with

$$g_k(\lambda, a, \sigma) \stackrel{\text{def}}{=} \mu_k(\lambda, \sigma)a_k - \lambda k^2\pi^2 (a^3)_k, \tag{27}$$

where

$$\mu_k = \mu_k(\lambda, \sigma) \stackrel{\text{def}}{=} -k^4\pi^4 + \lambda k^2\pi^2 - \lambda\sigma, \tag{28}$$

and

$$(a^3)_k \stackrel{\text{def}}{=} \sum_{\substack{k_1+k_2+k_3=k \\ k_i\in\mathbb{Z}\setminus\{0\}}} a_{|k_1|}a_{|k_2|}a_{|k_3|}.$$

The relations $a_k \in \mathbb{R}$, $a_0 = 0$ and $a_{-k} = a_k$ imply the new relations $g_k \in \mathbb{R}$, $g_{-k} = g_k$ and $g_0 = 0$. Hence, we only need to solve $g_k = 0$ for $k \geq 1$. Set $g \stackrel{\text{def}}{=} (g_k)_{k\geq 1}$.

Now consider the kernel equation associated to the steady states diblock copolymer equation:

$$D_u F(\lambda, u)[v] = -\left(v_{xx} + \lambda(v - 3u^2 v)\right)_{xx} - \lambda\sigma v = 0.$$

Plugging the cosine Fourier expansion of v

$$v(x) = \sum_{k\in\mathbb{Z}} b_k e^{ik\pi x} = 2\sum_{k\geq 1} b_k \cos(k\pi x),\ (b_k \in \mathbb{R},\ b_{-k} = b_k,\ b_0 = 0), \tag{29}$$

in $D_u F(\lambda, u)[v] = 0$ leads to $\sum_{k\in\mathbb{Z}} h_k e^{ik\pi x} = 0$, with

$$h_k(\lambda, a, b, \sigma) \stackrel{\text{def}}{=} \mu_k(\lambda, \sigma)b_k - 3\lambda k^2\pi^2 (a^2 b)_k, \tag{30}$$

where

$$(a^2 b)_k \stackrel{\text{def}}{=} \sum_{\substack{k_1+k_2+k_3=k \\ k_i\in\mathbb{Z}\setminus\{0\}}} a_{|k_1|}a_{|k_2|}b_{|k_3|}.$$

As above, the relations $h_k \in \mathbb{R}$, $h_{-k} = h_k$ and $h_0 = 0$ implies that we only need to solve $h_k = 0$ for $k \geq 1$.

Let $a \stackrel{\text{def}}{=} (a_k)_{k\geq 1}$, $b \stackrel{\text{def}}{=} (b_k)_{k\geq 1}$, $g \stackrel{\text{def}}{=} (g_k)_{k\geq 1}$ and $h \stackrel{\text{def}}{=} (h_k)_{k\geq 1}$.

Recall the definition of the extended operator $\mathcal{F}$ given in (11). We re-order the entries and consider

$$\mathcal{F}(\lambda, u, v) = \begin{pmatrix} \ell(v) - 1 \\ F(\lambda, u) \\ D_u F(\lambda, u)[v] \end{pmatrix}$$

where $\ell(v) = 1$ fixes the phase of the eigenvector v. Denote the vector of unknowns by

$$x = (\lambda, a, b).$$

Moving to Fourier space, and recalling (27) and (30), the functional equation $\mathcal{F}(\lambda, u, v) = 0$ becomes, for a fixed parameter value $\sigma \in \mathbb{R}$,

$$f(x, \sigma) \stackrel{\text{def}}{=} \begin{pmatrix} \eta(b) \\ g(\lambda, a, \sigma) \\ h(\lambda, a, b, \sigma) \end{pmatrix}, \tag{31}$$

where

$$\eta(b) \stackrel{\text{def}}{=} \frac{1}{\bar{b}_{k_0}} b_{k_0} - 1, \tag{32}$$

where the condition $\eta(b) = 0$ implies that we fix the k_0-th component of the eigenvector to be equal to a fixed value $\bar{b}_{k_0}$, as $\eta(b) = 0$ is equivalent to $b_{k_0} = \bar{b}_{k_0}$ The corresponding element ℓ in the dual space is $\ell(b) = \left(\frac{1}{\bar{b}_{k_0}}\right) e_{k_0} \cdot b$, where $(e_{k_0})_j = \delta_{k_0,j}$.

The Banach space on which we study the zeroes of f defined in (31) is

$$\mathbb{X} \stackrel{\text{def}}{=} \mathbb{R} \times \ell^1_\nu \times \ell^1_\nu, \tag{33}$$

endowed with the norm

$$\|x\|_{\mathbb{X}} \stackrel{\text{def}}{=} \max\left\{\frac{1}{\delta}|\lambda|, \|a\|_{1,\nu}, \|b\|_{1,\nu}\right\}, \tag{34}$$

where $\delta > 0$ is a weight and where

$$\ell^1_\nu \stackrel{\text{def}}{=} \{c = \{c_k\}_{k\geq 1} \,:\, \|c\|_{1,\nu} < \infty\}, \tag{35}$$

is equipped with a "weighted ell one norm"

$$\|c\|_{1,\nu} \stackrel{\text{def}}{=} 2\sum_{k\geq 1} |c_k|\nu^k = \sum_{k\in\mathbb{Z}\setminus\{0\}} |c_{|k|}|\nu^{|k|}, \tag{36}$$

for some fixed weight $\nu \geq 1$.

We solve the problem $f(x) = 0$ using the field of rigorous numerics (e.g. see [33]). This requires recalling some basic tools from functional analysis. Since all the results of the section are classical and can be found for instance in [16], we omit the proofs.

3.1. **Functional-analytic background.** We note that ℓ^1_ν defined in (35) is a Banach space and moreover has the property of being a Banach algebra under discrete convolution defined as

$$a * b = \left\{ \sum_{\substack{k_1,k_2\in\mathbb{Z}\setminus\{0\} \\ k_1+k_2=k}} a_{|k_1|} b_{|k_2|} \right\}_{k\geq 1}, \quad a = \{a_k\}_{k\geq 1}, b = \{b_k\}_{k\geq 1} \in \ell^1_\nu.$$

More explicitly, we have the following.

Lemma 3.1. *If $\nu \geq 1$ and $a, b \in \ell^1_\nu$, then $a * b \in \ell^1_\nu$ and*

$$\|a * b\|_{1,\nu} \leq \|a\|_{1,\nu}\|b\|_{1,\nu}. \tag{37}$$

For a sequence of real numbers $c = \{c_n\}_{n=1}^\infty$ define the ν^{-1}-weighted supremum norm

$$\|c\|_{\infty,\nu^{-1}} \stackrel{\text{def}}{=} \frac{1}{2}\sup_{n\geq 1}|c_n|\left(\frac{1}{\nu}\right)^n, \tag{38}$$

and let

$$\ell^\infty_{\nu^{-1}} \stackrel{\text{def}}{=} \left\{c = \{c_n\}_{n=1}^\infty : \|c\|_{\infty,\nu^{-1}} < \infty\right\}.$$

From the definition of the norm in (38), it follows that given $c \in \ell^\infty_{\nu^{-1}}$,

$$|c_n| \le 2\nu^n \|c\|_{\infty,\nu^{-1}}, \quad \forall\ n \ge 1. \tag{39}$$

Then, given $a \in \ell^1_\nu$ and $c \in \ell^\infty_{\nu^{-1}}$, we conclude by (39) that

$$\left|\sum_{k\ge1} c_k a_k\right| \le \sum_{k\ge1} |c_k||a_k| \le \|c\|_{\infty,\nu^{-1}} \left(2\sum_{k\ge1}|a_k|\nu^k\right) = \|c\|_{\infty,\nu^{-1}}\|a\|_{1,\nu}. \tag{40}$$

This bound is used to estimate linear operators of the following type. Denote by $B(V,W)$ the space of bounded linear operators acting between a Banach space V and a Banach space W, and denote $\|\cdot\|_{B(V,W)}$ the operator norm.

Corollary 3.2. *Let $M^{(m)} = \{M_{k,n}\}_{k,n=1,\dots,m-1}$ be an $(m-1)\times(m-1)$ matrix, $\{\mu_n\}_{n=m}^\infty$ be a sequence of numbers with*

$$|\mu_n| \le |\mu_m|,$$

for all $n \ge m$, and $M\colon \ell^1_\nu \to \ell^1_\nu$ be the linear operator defined by

$$Mb = \begin{pmatrix} M^{(m)} & & 0 \\ & \mu_m & \\ 0 & & \mu_{m+1} \\ & & & \ddots \end{pmatrix} \begin{bmatrix} b^{(m)} \\ b_m \\ b_{m+1} \\ \vdots \end{bmatrix}.$$

Here $b^{(m)} = (b_1,\dots,b_{m-1})^T \in \mathbb{R}^{m-1}$. Then $M \in B(\ell^1_\nu,\ell^1_\nu)$ is a bounded linear operator and

$$\|M\|_{B(\ell^1_\nu,\ell^1_\nu)} = \max(K, |\mu_m|), \tag{41}$$

where

$$K \stackrel{\text{def}}{=} \max_{1\le n\le m-1} \frac{1}{\nu^n}\sum_{k=1}^{m-1}|M_{k,n}|\nu^k. \tag{42}$$

Lemma 3.3. *Given $\nu \ge 1$, $k \ge 1$ and $a \in \ell^1_\nu$, the function $l^k_a\colon \ell^1_\nu \to \mathbb{R}$ defined by*

$$l^k_a(h) \stackrel{\text{def}}{=} (a*h)_k = \sum_{\substack{k_1+k_2=k \\ k_1,k_2\in\mathbb{Z}\setminus\{0\}}} a_{|k_1|}h_{|k_2|}$$

with $h \in \ell^1_\nu$, is a bounded linear functional, and

$$\|l^k_a\| = \sup_{\|h\|_{1,\nu}\le1} \left|l^k_a(h)\right| \le \frac{1}{2}\sup_{j\ge1}\frac{(a_{|k+j|}+a_{|k-j|})}{\nu^j}. \tag{43}$$

Fix a truncation mode to be m. Given $h \in \ell^1_\nu$, set

$$h^{(m)} \stackrel{\text{def}}{=} (h_1,\dots,h_{m-1},0,0,\dots) \in \ell^1_\nu$$
$$h^{(I)} \stackrel{\text{def}}{=} h - h^{(m)} \in \ell^1_\nu.$$

Corollary 3.4. *Let $N \in \mathbb{N}$ and let $\bar\alpha = (\bar\alpha_1,\dots,\bar\alpha_N,0,0,\dots) \in \ell^1_\nu$. Suppose that $1 \le k < m$ and define $\hat l^k_{\bar\alpha} \in (\ell^1_\nu)^*$ by*

$$\hat l^k_{\bar\alpha}(h) \stackrel{\text{def}}{=} (\bar\alpha * h^{(I)})_k = \sum_{\substack{k_1+k_2=k \\ k_1,k_2\in\mathbb{Z}\setminus\{0\}}} \bar\alpha_{|k_1|}h^{(I)}_{|k_2|}.$$

Then, for all $h \in \ell^1_\nu$ such that $\|h\|_{1,\nu} \le 1$,

$$\left|\hat l^k_{\bar\alpha}(h)\right| \le \Psi_k(\bar\alpha) \stackrel{\text{def}}{=} \max\left(\max_{m\le j\le N-k}\frac{|\bar\alpha_{k+j}|}{\nu^j}, \max_{m\le j\le k+N}\frac{|\bar\alpha_{|k-j|}|}{\nu^j}\right). \tag{44}$$

3.2. **The general rigorous computational method.** We now present a general method to prove existence and compute global smooth solution curves of the equation $f(x,\sigma)=0$ in the Banach space X as defined in (33). The method is based on the radii polynomial approach, first introduced in [11]. The version of the approach we use here is a direct application of the work [7] and is strongly influenced by the rigorous branch following method of [34]. The idea is to compute a set of numerical approximations $\{\bar{x}_0,\dots,\bar{x}_j\}$ of $f(x,\sigma)=0$ at the parameter values $\{\sigma_0,\dots,\sigma_j\}$ by considering a finite dimensional projection, to use the approximations to construct a global continuous curve of piecewise linear interpolations between the $\bar{x}_i$'s and to apply the uniform contraction theorem on *tubes* centered at each segment to conclude about the existence of a unique smooth solution curve of $f=0$ nearby the piecewise linear curve of approximations.

3.2.1. *Construction of a Piecewise Linear Curve of Approximations.* To construct a piecewise linear curve of approximations of $f(x,\sigma)=0$, we consider a finite dimensional projection $f^{(m)}$ of f whose dimension depends on m. Given $c=(c_k)_{k\geq 1}\in\ell^1_\nu$ denote by $c^{(m)}=(c_1,\dots,c_{m-1})\in\mathbb{R}^{m-1}$ a finite part of c of size $m-1$. Denote $x^{(m)}=(\lambda,a^{(m)},b^{(m)})\in\mathbb{R}^{2m-1}$. In the remaining of the section, $(\cdot)^{(m)}$ denotes considering this finite dimensional projection. Reversely, when we have some finite dimensional vector $x^{(m)}$, x denotes the infinite vector obtained by completing $x^{(m)}$ with zeros.

Consider a finite dimensional projection $f^{(m)}$ of (31) given by

$$f^{(m)}(x^{(m)},\sigma)=\begin{pmatrix}\eta(x^{(m)})\\ g^{(m)}(x^{(m)},\sigma)\\ h^{(m)}(x^{(m)},\sigma)\end{pmatrix}, \tag{45}$$

where $g^{(m)}(x^{(m)},\sigma)\in\mathbb{R}^{m-1}$ (resp. $h^{(m)}$) corresponds to the finite part of g (resp. h) of size $m-1$. We have that $f^{(m)}:\mathbb{R}^{2m-1}\times\mathbb{R}\to\mathbb{R}^{2m-1}$. Assume that using a standard parameter continuation (i.e. a predictor-corrector algorithm based on Newton's method) in σ, we compute a set $\{\bar{x}_0,\dots,\bar{x}_j\}$ of approximations at the parameter values $\{\sigma_0,\dots,\sigma_j\}$ respectively that defines a piecewise linear approximation curve (see Figure 5). The next step is to show existence of a unique smooth solution curve $\mathcal{C}$ of $f=0$ nearby the piecewise linear curve of approximations, as portrayed in Figure 5. This task is twofold. First, one shows the existence of a unique portion of solution curve $\mathcal{C}^{(i)}$ in a small *tube* centered at the segment $\{(1-s)\bar{x}_i+s\bar{x}_{i+1}\mid s\in[0,1]\}$. This is done in Theorem 3.5. Second, one shows that

$$\mathcal{C}\overset{\text{def}}{=}\bigcup_{i=0}^{j-1}\mathcal{C}^{(i)}$$

is a global continuous solution curve of $f(x,\sigma)=0$.

3.2.2. *Uniform Contraction and the Radii Polynomial Approach.* Let us define what is required to prove existence of some portion of curve $\mathcal{C}^{(i)}$. Without loss of generality, let us introduce the idea to prove the existence of $\mathcal{C}^{(0)}$ that is the piece of curve close to the segment $[\bar{x}_0,\bar{x}_1]$. For any s in $[0,1]$, we set

$$\bar{x}_s\overset{\text{def}}{=}(1-s)\bar{x}_0+s\bar{x}_1=\bar{x}_0+s\Delta\bar{x},\ \text{where }\Delta\bar{x}\overset{\text{def}}{=}\bar{x}_1-\bar{x}_0 \tag{46}$$

$$\sigma_s\overset{\text{def}}{=}(1-s)\sigma_0+s\sigma_1=\sigma_0+s\Delta\sigma,\ \text{where }\Delta\sigma\overset{\text{def}}{=}\sigma_1-\sigma_0. \tag{47}$$

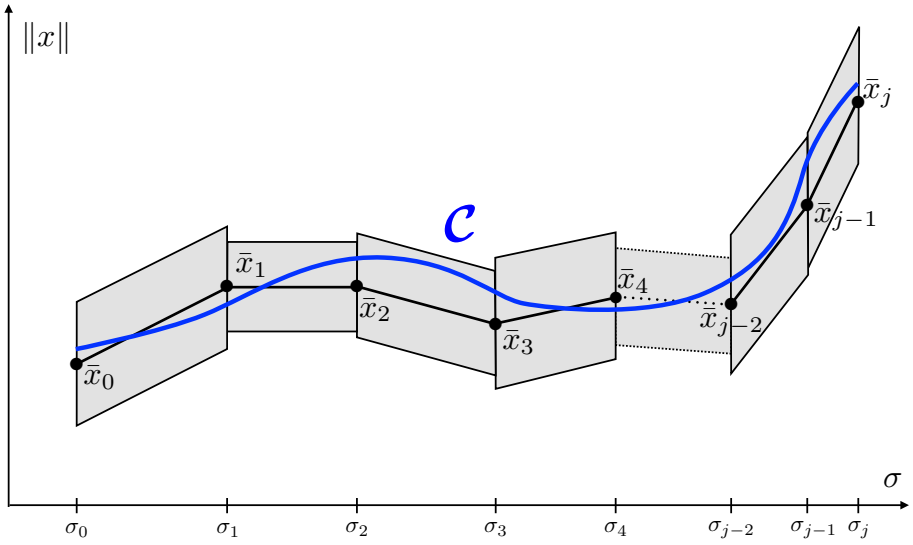

FIGURE 5. Piecewise linear curve approximation (in black) constructed using parameter continuation and existence of a global solution curve $\mathcal{C}$ of $f = 0$ (in blue) nearby the approximations

Then we define, still for s in $[0, 1]$, the Newton-like operator

$$T_s(x) \stackrel{\text{def}}{=} x - Af(x, \sigma_s), \tag{48}$$

where A is an injective linear operator approximating the inverse of $Df(\bar{x}_0, \sigma_0)$. Denote $\bar{x}_0 = (\bar{\lambda}_0, \bar{a}_0, \bar{b}_0)$. In the sequel, we use the notation $x = (x_1, x_2, x_3)$ with $x_1 = \lambda$, $x_2 = a$ and $x_3 = b$. To obtain the operator A, assume that

- the Jacobian matrix $Df^{(m)}(\bar{x}_0, \sigma_0)$ has been computed;
- an approximate inverse $A^{(m)}$ of $Df^{(m)}(\bar{x}_0, \sigma_0)$ has been computed;
- $A^{(m)}$ is injective. In practice, showing that $\|I - A^{(m)}Df^{(m)}(\bar{x}_0, \sigma_0)\| < 1$ is sufficient to prove that $A^{(m)}$ is injective.

Denote $A^{(m)}$ block-wise as

$$A^{(m)} = \begin{bmatrix} A_{11}^{(m)} & A_{12}^{(m)} & A_{13}^{(m)} \\ A_{21}^{(m)} & A_{22}^{(m)} & A_{23}^{(m)} \\ A_{31}^{(m)} & A_{32}^{(m)} & A_{33}^{(m)} \end{bmatrix} \in \mathbb{R}^{(2m-1)\times(2m-1)}, \tag{49}$$

with $A_{11}^{(m)} \in \mathbb{R}$, $A_{1j}^{(m)} \in \mathbb{R}^{1\times(m-1)}$ for $j = 2, 3$, $A_{i1}^{(m)} \in \mathbb{R}^{(m-1)\times 1}$ for $i = 2, 3$ and $A_{ij}^{(m)} \in \mathbb{R}^{(m-1)\times(m-1)}$ for $2 \leq i, j \leq 3$. The operator A which acts as an approximate inverse for

$$Df(\bar{x}_0, \sigma_0) = \begin{bmatrix} \partial_\lambda \eta(\bar{x}_0) & D_a\eta(\bar{x}_0) & D_b\eta(\bar{x}_0) \\ \partial_\lambda g(\bar{x}_0, \sigma_0) & D_a g(\bar{x}_0, \sigma_0) & D_b g(\bar{x}_0, \sigma_0) \\ \partial_\lambda h(\bar{x}_0, \sigma_0) & D_a h(\bar{x}_0, \sigma_0) & D_b h(\bar{x}_0, \sigma_0) \end{bmatrix}$$

is given block-wise by

$$A = \begin{bmatrix} A_{11} & A_{12} & A_{13} \\ A_{21} & A_{22} & A_{23} \\ A_{31} & A_{32} & A_{33} \end{bmatrix}, \tag{50}$$

where

- $A_{11} = A_{11}^{(m)} \in \mathbb{R}$;
- $A_{1j} \in B\left(\ell^1_\nu, \mathbb{R}\right)$ for $2 \le j \le 3$: for $x_j \in \ell^1_\nu$, $A_{1j}x_j = A_{1j}^{(m)} x_j^{(m)} \in \mathbb{R}$;
- $A_{i1} \in \ell^1_\nu$ for $2 \le i \le 3$: for $x_1 \in \mathbb{R}$, $A_{i1}x_1 = (A_{i1}^{(m)} x_1, 0_\infty) \in \ell^1_\nu$;
- $A_{ij} \in B\left(\ell^1_\nu, \ell^1_\nu\right)$ for $2 \le i, j \le 3$: for $x_j \in \ell^1_\nu$,

$$(A_{ij}x_j)_k = \begin{cases} (A_{ij}^{(m)} x_j^{(m)})_k, & k = 1, \dots, m-1, \\ \delta_{i,j} \dfrac{1}{\mu_k(\bar{\lambda}_0, \sigma_0)} (x_j)_k, & k \ge m, \end{cases}$$

  where $\delta_{i,j}$ equals 1 if $i = j$ and 0 otherwise.

Combining the above, A is a linear operator which acts on $x = (x_1, x_2, x_3) \in \mathbb{X}$ component-wise as

$$(Ax)_i = \sum_{j=1}^{3} A_{ij}x_j,$$

with $(Ax)_1 \in \mathbb{R}$ and $(Ax)_i \in \ell^1_\nu$, for $i = 2, 3$.

Moreover, define the linear operator

$$A^\dagger = \begin{bmatrix} 0 & 0 & A_{13}^\dagger \\ A_{21}^\dagger & A_{22}^\dagger & 0 \\ A_{31}^\dagger & A_{32}^\dagger & A_{33}^\dagger \end{bmatrix},$$

which acts on $c = (c_1, c_2, c_3)$ component-wise as

$$\begin{aligned} (A^\dagger c)_1 &= A_{13}^\dagger c_3 \overset{\text{def}}{=} D_b \eta(\bar{x}_0) c_3 \\ (A^\dagger c)_2 &= \sum_{j=1}^{3} A_{2j}^\dagger c_j \overset{\text{def}}{=} \partial_\lambda g^{(m)}(\bar{x}_0, \sigma_0) c_1 + A_{22}^\dagger c_2 \\ (A^\dagger c)_3 &= \sum_{j=1}^{3} A_{3j}^\dagger c_j \overset{\text{def}}{=} \partial_\lambda h^{(m)}(\bar{x}_0, \sigma_0) c_1 + A_{32}^\dagger c_2 + A_{33}^\dagger c_3 \end{aligned}$$

where for $i, j = 2, 3$, $A_{i,j}^\dagger c_j$ is defined component-wise by

$$\left(A_{22}^\dagger c_2\right)_k = \begin{cases} \left(D_a g^{(m)}(\bar{x}_0, \sigma_0) c_2^{(m)}\right)_k, & 1 \le k < m \\ \mu_k(\bar{\lambda}_0, \sigma_0)(c_2)_k, & k \ge m \end{cases}$$

$$\left(A_{32}^\dagger c_2\right)_k = \begin{cases} \left(D_a h^{(m)}(\bar{x}_0, \sigma_0) c_2^{(m)}\right)_k, & 1 \le k < m \\ 0, & k \ge m \end{cases}$$

$$\left(A_{33}^\dagger c_3\right)_k = \begin{cases} \left(D_b h^{(m)}(\bar{x}_0, \sigma_0) c_3^{(m)}\right)_k, & 1 \le k < m \\ \mu_k(\bar{\lambda}_0, \sigma_0)(c_3)_k, & k \ge m. \end{cases}$$

The operator $A^\dagger$ acts as an approximation for $D_x f(\bar{x}_0, \sigma_0)$, and is used in the radii polynomial approach, which we now present. A more detailed proof can be found for instance in [19, 20].

Theorem 3.5 (**Radii Polynomial Approach**). *Recall the definitions of f, $\bar{x}_s$, σ_s and A, given respectively in (31), (46), (47) and (50). Let $Y_0, Z_0, Z_1, Z_2 \ge 0$ be*

bounds satisfying

$$\|Af(\bar{x}_s,\sigma_s)\|_{\mathbb{X}} \leq Y_0, \quad \forall\ s\in[0,1] \tag{51}$$

$$\|I - AA^{\dagger}\|_{B(\mathbb{X},\mathbb{X})} \leq Z_0 \tag{52}$$

$$\|A[D_x f(\bar{x}_0,\sigma_0) - A^{\dagger}]\|_{B(\mathbb{X},\mathbb{X})} \leq Z_1 \tag{53}$$

$$\|A[D_x f(\bar{x}_s+b,\sigma_s) - D_x f(\bar{x}_0,\sigma_0)]\|_{B(\mathbb{X},\mathbb{X})} \leq Z_2(r), \quad \forall\ b\in B_r(0) \text{ and } \forall\ s\in[0,1]. \tag{54}$$

Define the radii polynomial

$$p(r) \overset{\text{def}}{=} Z_2(r)r + (Z_1 + Z_0 - 1)r + Y_0. \tag{55}$$

If there exists $r_0 > 0$ *such that*

$$p(r_0) < 0,$$

then there exists a C^∞ *function*

$$\tilde{x} : [0,1] \to \bigcup_{s\in[0,1]} B_{r_0}(\bar{x}_s)$$

such that

$$f(\tilde{x}(s),\sigma_s) = 0, \quad \forall\ s\in[0,1].$$

Furthermore, these are the only solutions in the tube $\bigcup_{s\in[0,1]} B_{r_0}(\bar{x}_s)$.

Proof. The idea is to prove that for every $s\in[0,1]$, the operator T_s defined in (48) satisfies first that $T_s : B_{r_0}(\bar{x}_s) \to B_{r_0}(\bar{x}_s)$ and then that T_s is a contraction. For each $s\in[0,1]$, the contraction mapping theorem implies the existence of a unique $\tilde{x}(s)\in B_{r_0}(\bar{x}_s)$ such that $f(\tilde{x}(s),\sigma_s) = 0$. The fact that the function $\tilde{x}(s)$ is C^∞ follows from an application of the uniform contraction principle on the mapping

$$\tilde{T} : \begin{cases} [0,1]\times B_r(0) \longrightarrow B_r(0) \\ (s,w) \longmapsto \tilde{T}(s,w) \overset{\text{def}}{=} w - Af(w+\bar{x}_s,\sigma_s). \end{cases}$$

□

3.3. **The radii polynomial for saddle-node bifurcations.** Recall that by considering a Galerkin projection $f^{(m)} : \mathbb{R}^{2m-1}\times\mathbb{R}\to\mathbb{R}^{2m-1}$, one computed two solutions $\bar{x}_0 = (\bar{\lambda}_0,\bar{a}_0,\bar{b}_0)$ at σ_0 and $\bar{x}_1 = (\bar{\lambda}_1,\bar{a}_1,\bar{b}_1)$ at σ_1 such that $f^{(m)}(\bar{x}_0,\sigma_0)\approx 0$ and $f^{(m)}(\bar{x}_1,\sigma_1)\approx 0$. Denote

$$\Delta\bar{x} = \bar{x}_1 - \bar{x}_0 = (\bar{\lambda}_1 - \bar{\lambda}_0, \bar{a}_1 - \bar{a}_0, \bar{b}_1 - \bar{b}_0) = (\Delta\bar{\lambda},\Delta\bar{a},\Delta\bar{b}) \text{ and } \Delta\sigma = \sigma_1 - \sigma_0.$$

In order to apply the radii polynomial approach (Theorem 3.5) to the problem (31), we compute the bounds Y_0, Z_0, Z_1 and $Z_2(r)$ satisfying (51), (52), (53) and (54), respectively.

3.3.1. *The bound* $\mathbf{Y_0}$. Recall that the bound Y_0 satisfies the inequality (51). Denote $\xi_s = (\bar{\lambda}_s,\bar{a}_s,\bar{b}_s,\sigma_s)$ and $\xi = (\lambda,a,b,\sigma)$. Since $\xi_s = \xi_0 + s(\xi_1 - \xi_0)$, then using Taylor's theorem

$$Af(\bar{x}_s,\sigma_s) = Af(\xi_s) = Af(\xi_0) + sAD_\xi f(\xi_0)(\xi_1-\xi_0) + R(\xi_s),$$

where $f(\xi_0) = f(\bar{x}_0,\sigma_0)$, $D_\xi f(\xi_0)(\xi_1-\xi_0) = D_x f(\bar{x}_0,\sigma_0)\Delta\bar{x} + \frac{\partial f}{\partial\sigma}(\bar{x}_0,\sigma_0)\Delta\sigma$, and

$$\begin{aligned} \|R(\xi_s)\|_{\mathbb{X}} &\leq \sup_{s,t\in[0,1]} \|\frac{s^2}{2} AD_\xi^2 f(\xi_t)(\xi_1-\xi_0,\xi_1-\xi_0)\|_{\mathbb{X}} \\ &= \frac{1}{2}\sup_{t\in[0,1]} \|AD_\xi^2 f(\xi_t)(\xi_1-\xi_0,\xi_1-\xi_0)\|_{\mathbb{X}} \end{aligned}$$

Recalling (46), (47), $\xi_1 - \xi_0 = (\bar\lambda_1, \bar a_1, \bar b_1, \sigma_1) - (\bar\lambda_0, \bar a_0, \bar b_0, \sigma_0) = (\bar x_1 - \bar x_0, \sigma_1 - \sigma_0) = (\Delta\bar x, \Delta\sigma)$. Note that

$$D^2_\xi f(\xi_t)(\xi_1-\xi_0,\xi_1-\xi_0) = \begin{pmatrix} 0 \\ D^2_\xi g(\xi_t)(\xi_1-\xi_0,\xi_1-\xi_0) \\ D^2_\xi h(\xi_t)(\xi_1-\xi_0,\xi_1-\xi_0) \end{pmatrix}, \tag{56}$$

where

$$\begin{aligned}
\left(D^2_\xi g(\xi_t)(\xi_1-\xi_0,\xi_1-\xi_0)\right)_k &= -2\Delta\bar\lambda\Delta\sigma(\bar a_t)_k + 2(k^2\pi^2\Delta\bar\lambda - \Delta\bar\lambda\sigma_t - \Delta\sigma\bar\lambda_t)(\Delta\bar a)_k \\
&\quad - 6k^2\pi^2\left(\Delta\bar\lambda(\bar a_t^2\Delta\bar a)_k + \bar\lambda_t(\Delta\bar a^2\bar a_t)_k\right) \\
\left(D^2_\xi h(\xi_t)(\xi_1-\xi_0,\xi_1-\xi_0)\right)_k &= -2\Delta\bar\lambda\Delta\sigma(\bar b_t)_k + 2(k^2\pi^2\Delta\bar\lambda - \Delta\bar\lambda\sigma_t - \Delta\sigma\bar\lambda_t)(\Delta\bar b)_k \\
&\quad - 6k^2\pi^2\left(\Delta\bar\lambda(\bar a_t^2\Delta\bar b)_k + \bar\lambda_t(\Delta\bar a^2\bar b_t)_k\right) \\
&\quad - 12k^2\pi^2\left(\Delta\bar\lambda(\bar a_t\bar b_t\Delta\bar a)_k + \bar\lambda_t(\bar a_t\Delta\bar a\Delta\bar b)_k\right).
\end{aligned}$$

Using interval arithmetic, one can easily compute bounds $Y_0^{(0)}, Y_0^{(1)}$ and $Y_0^{(2)}$ such that

$$\begin{aligned}
\|Af(\xi_0)\|_{\mathbb{X}} &\le Y_0^{(0)} \\
\|AD_\xi f(\xi_0)(\xi_1-\xi_0)\|_{\mathbb{X}} &\le Y_0^{(1)} \\
\frac{1}{2}\sup_{t\in[0,1]}\|AD^2_\xi f(\xi_t)(\xi_1-\xi_0,\xi_1-\xi_0)\|_{\mathbb{X}} &\le Y_0^{(2)}
\end{aligned}$$

and finally set

$$Y_0 \stackrel{\text{def}}{=} Y_0^{(0)} + Y_0^{(1)} + Y_0^{(2)}. \tag{57}$$

3.3.2. *The bound* $\boldsymbol{Z_0}$. Let $B \stackrel{\text{def}}{=} I - AA^\dagger$, which we express as

$$B = \begin{bmatrix} B_{11} & B_{12} & B_{13} \\ B_{21} & B_{22} & B_{23} \\ B_{31} & B_{32} & B_{33} \end{bmatrix}.$$

Setting

$$Z_0 \stackrel{\text{def}}{=} \max\left\{ |B_{11}| + \frac{1}{\delta}\sum_{j=2}^{3}\|B_{1j}\|_{\infty,\nu^{-1}} \ , \ \max_{i=2,3}\left(\delta\|B_{i1}\|_{1,\nu} + \sum_{j=2}^{3}\|B_{ij}\|_{B(\ell^1_\nu,\ell^1_\nu)}\right)\right\} \tag{58}$$

satisfies the bound (52).

3.3.3. *The bound* $\boldsymbol{Z_1}$. Given $h = (h_1, h_2, h_3) \in B_1(0) \subset \mathbb{X}$ let

$$z = z(h) \stackrel{\text{def}}{=} [D_x f(\bar x_0, \sigma_0) - A^\dagger]h,$$

which we denote as $z = (z_1, z_2, z_3)$. Note that $z_1 = 0$ and that

$$(z_2)_k = \begin{cases} -3\bar\lambda_0 k^2\pi^2\left(\bar a_0^2 h_2^{(I)}\right)_k, & 1 \le k < m \\ -3\bar\lambda_0 k^2\pi^2\left(\bar a_0^2 h_2\right)_k - k^2\pi^2\left(\bar a_0^3\right)_k h_1, & k \ge m \end{cases} \tag{59}$$

$$(z_3)_k = \begin{cases} -3\bar\lambda_0 k^2\pi^2\left(\bar a_0^2 h_3^{(I)}\right)_k - 6\bar\lambda_0 k^2\pi^2\left(\bar a_0\bar b_0 h_2^{(I)}\right)_k, & 1 \le k < m \\ -3\bar\lambda_0 k^2\pi^2\left(\bar a_0^2 h_3\right)_k - 6\bar\lambda_0 k^2\pi^2\left(\bar a_0\bar b_0 h_2\right)_k - 3k^2\pi^2\left(\bar a_0^2\bar b_0\right)_k h_1, & k \ge m\,. \end{cases} \tag{60}$$

Using Corollary 3.4, we get that for $1 \le k < m$,

$$|(z_2)_k| \le (\hat{z}_2)_k \stackrel{\text{def}}{=} 3|\bar{\lambda}_0| k^2\pi^2 \Psi_k(|\bar{a}_0|^2)$$
$$|(z_3)_k| \le (\hat{z}_3)_k \stackrel{\text{def}}{=} 3|\bar{\lambda}_0| k^2\pi^2 \left(\Psi_k(|\bar{a}_0|^2) + 2\Psi_k(|\bar{a}_0\bar{b}_0|^2)\right).$$

The following elementary result is useful to bound the tail quantities involved in z_2 and z_3.

Lemma 3.6. *Let $\gamma_1 \ge 0$ and assume that the projection dimension m satisfies*

$$m > \frac{\sqrt{\bar{\lambda}_0}}{\pi}. \tag{61}$$

Then, for all $k \ge m$,

$$\left|\frac{\gamma_1 k^2\pi^2}{\mu_k(\bar{\lambda}_0, \sigma_0)}\right| \le \frac{\gamma_1}{m^2\pi^2 - \bar{\lambda}_0}. \tag{62}$$

Proof. Since $m > \frac{\sqrt{\bar{\lambda}_0}}{\pi}$, for all $k \ge m$, $|\mu_k(\bar{\lambda}_0, \sigma_0)| = k^4\pi^4 - \bar{\lambda}_0 k^2\pi^2 + \bar{\lambda}_0\sigma_0 > 0$. Then,

$$\left|\frac{\gamma_1 k^2\pi^2}{\mu_k(\bar{\lambda}_0, \sigma_0)}\right| = \frac{\gamma_1 k^2\pi^2}{k^4\pi^4 - \bar{\lambda}_0 k^2\pi^2 + \bar{\lambda}_0\sigma_0} = \frac{\gamma_1}{k^2\pi^2 - \bar{\lambda}_0 + \frac{\bar{\lambda}_0\sigma_0}{k^2\pi^2}} \le \frac{\gamma_1}{m^2\pi^2 - \bar{\lambda}_0}. \qquad \square$$

Combining Corollary 3.4 with Lemma 3.6, and under the assumption (61), we get that for any $h \in B_1(0) \subset \mathbb{X}$,

$$\frac{1}{\delta}|A_{1,2}z_2(h)| \le \zeta_{1,2} \stackrel{\text{def}}{=} \frac{1}{\delta}\left|A^{(m)}_{1,2}\right| \cdot \hat{z}^{(m)}_2 \quad \text{and} \quad \frac{1}{\delta}|A_{1,3}z_3(h)| \le \zeta_{1,3} \stackrel{\text{def}}{=} \frac{1}{\delta}\left|A^{(m)}_{1,3}\right| \cdot \hat{z}^{(m)}_3$$

and for $i = 2, 3$,

$$\begin{aligned}
\|A_{i,2}z_2(h)\|_{1,\nu} \quad &\le \quad \zeta_{i,2} \stackrel{\text{def}}{=} 2\sum_{k=1}^{m-1}\left|\left((A^{(m)}_{i,2})\hat{z}^{(m)}_2\right)_k\right|\nu^k \\
&\qquad + \ \delta_{i,2}\frac{(\|\bar{a}_0\|_{1,\nu})^2}{m^2\pi^2 - \bar{\lambda}_0}\left(3|\bar{\lambda}_0| + \delta\|\bar{a}_0\|_{1,\nu}\right) \\
\|A_{i,3}z_3(h)\|_{1,\nu} \quad &\le \quad \zeta_{i,3} \stackrel{\text{def}}{=} 2\sum_{k=1}^{m-1}\left|\left((A^{(m)}_{i,3})\hat{z}^{(m)}_3\right)_k\right|\nu^k + \delta_{i,3}\frac{3\|\bar{a}_0\|_{1,\nu}}{m^2\pi^2 - \bar{\lambda}_0}\left(|\bar{\lambda}_0|\|\bar{a}_0\|_{1,\nu}\right. \\
&\qquad \left. +2|\bar{\lambda}_0|\|\bar{b}_0\|_{1,\nu} + \delta\|\bar{a}_0\|_{1,\nu}\|\bar{b}_0\|_{1,\nu}\right).
\end{aligned}$$

Using the previous bounds, we conclude that

$$\begin{aligned}
&\|A[D_x f(\bar{x}_0, \sigma_0) - A^\dagger]\|_{B(\mathbb{X},\mathbb{X})} \quad = \sup_{h\in B_1(0)} \|A[D_x f(\bar{x}_0, \sigma_0) - A^\dagger]h\|_{\mathbb{X}} \\
&= \sup_{h\in B_1(0)} \|Az(h)\|_{\mathbb{X}} \\
&\le \sup_{h\in B_1(0)} \max\left(\frac{1}{\delta}\left|\sum_{j=2}^{3} A_{1,j}z_j(h)\right| \ , \ \left\|\sum_{j=2}^{3} A_{2,j}z_j(h)\right\|_{1,\nu} \ , \ \left\|\sum_{j=2}^{3} A_{3,j}z_j(h)\right\|_{1,\nu}\right) \\
&\qquad \le Z_1 \stackrel{\text{def}}{=} \max_{i=1,2,3}\left(\zeta_{i,2} + \zeta_{i,3}\right),
\end{aligned} \tag{63}$$

3.3.4. *The bound* $\boldsymbol{Z_2}$. Recall that we look for a bound Z_2 satisfying (54). Fix $b \in B_r(0)$ and $s \in [0,1]$. Applying the Mean Value Inequality three times yields

$$\begin{aligned}
&\|A[D_x f(\bar{x}_s + b, \sigma_s) - D_x f(\bar{x}_0, \sigma_0)]\|_{B(\mathbb{X},\mathbb{X})} \\
&\quad \le \|A[D_x f(\bar{x}_s + b, \sigma_s) - D_x f(\bar{x}_s, \sigma_s)]\|_{B(\mathbb{X},\mathbb{X})} \\
&\qquad + \|A[D_x f(\bar{x}_s, \sigma_s) - D_x f(\bar{x}_0, \sigma_s)]\|_{B(\mathbb{X},\mathbb{X})} \\
&\qquad + \|A[D_x f(\bar{x}_0, \sigma_s) - D_x f(\bar{x}_0, \sigma_0)]\|_{B(\mathbb{X},\mathbb{X})} \\
&\quad \le \sup_{\substack{w \in B_r(\bar{x}_s) \\ u,v \in B_1(0) \\ s \in [0,1]}} \|AD_x^2 f(w, \sigma_s)(u,v)\|_{\mathbb{X}} r + \sup_{\substack{s,t \in [0,1] \\ u,v \in B_1(0)}} \|AD_x^2 f(\bar{x}_t, \sigma_s)(u,v)\|_{\mathbb{X}} \|\bar{x}_1 - \bar{x}_0\|_{\mathbb{X}} \\
&\qquad + \sup_{\substack{t \in [0,1] \\ v \in B_1(0)}} \|AD_{x,\sigma} f(\bar{x}_0, \sigma_t)v\|_{\mathbb{X}} |\sigma_1 - \sigma_0|.
\end{aligned}$$

Define Λ the (unbounded) diagonal operator

$$(\Lambda a)_k = k^2 \pi^2 a_k. \tag{64}$$

Given $u = (\lambda^u, a^u, b^u), v = (\lambda^v, a^v, b^v), w = (\lambda^w, a^w, b^w) \in \mathbb{X}$, a straightforward computation yields that $D_x^2 f(w, \sigma_s)(u,v) \in \mathbb{X}$ satisfies

$$\begin{aligned}
\left(D_x^2 f(w, \sigma_s)(u,v)\right)_1 &= 0 \\
\left(D_x^2 f(w, \sigma_s)(u,v)\right)_2 &= D_x^2 g(w, \sigma_s)(u,v) \\
&= (\Lambda - \sigma_s I)(\lambda^u a^v + \lambda^v a^u) \\
&\quad - 3\Lambda \left(\lambda^u (a^w)^2 a^v + \lambda^v (a^w)^2 a^u + 2\lambda^w a^w a^u a^v\right) \\
\left(D_x^2 f(w, \sigma_s)(u,v)\right)_3 &= D_x^2 h(w, \sigma_s)(u,v) \\
&= (\Lambda - \sigma_s I)(\lambda^u b^v + \lambda^v b^u) \\
&\quad - 3\Lambda \left(\lambda^u (2a^w a^v b^w + (a^w)^2 b^v) + \lambda^v (2a^w a^u b^w + (a^w)^2 b^u)\right) \\
&\quad - 6\Lambda \lambda^w \left(a^u a^v b^w + a^u a^w b^v + a^w a^v b^u\right).
\end{aligned}$$

Hence, for $i = 1, 2, 3$, and given $u, v \in B_1(0)$ and any $w = (\lambda^w, a^w, b^w) \in \mathbb{X}$,

$$\begin{aligned}
\left\|A_{i,2} D_x^2 g(w, \sigma_s)(u,v)\right\|^{(i)} &\le \hat{\alpha}_{i,2}(w) \stackrel{\text{def}}{=} 2\delta \alpha_{i,2}^{(1)} + 6\alpha_{i,2}^{(2)} \|a^w\|_{1,\nu} \left(\delta \|a^w\|_{1,\nu} + |\lambda^w|\right) \\
\left\|A_{i,3} D_x^2 h(w, \sigma_s)(u,v)\right\|^{(i)} &\le \hat{\alpha}_{i,3}(w) \stackrel{\text{def}}{=} 2\delta \alpha_{i,3}^{(1)} + 3\alpha_{i,3}^{(2)} \big(4\delta \|a^w\|_{1,\nu} \|b^w\|_{1,\nu} \\
&\qquad + 2\delta \|a^w\|_{1,\nu}^2 + 2|\lambda^w| (\|b^w\|_{1,\nu} + 2\|a^w\|_{1,\nu})\big)
\end{aligned}$$

where $\|\cdot\|^{(1)} = |\cdot|$ and $\|\cdot\|^{(i)} = \|\cdot\|_{1,\nu}$ for $i, j = 2, 3$, and where

$$\begin{aligned}
\alpha_{1,j}^{(1)} &\stackrel{\text{def}}{=} \sup_{s \in [0,1]} \|A_{1,j}(\Lambda - \sigma_s I)\|_{\infty,\nu^{-1}}, \qquad \alpha_{1,j}^{(2)} \stackrel{\text{def}}{=} \|A_{1,j}\Lambda\|_{\infty,\nu^{-1}} \\
\alpha_{i,j}^{(1)} &\stackrel{\text{def}}{=} \sup_{s \in [0,1]} \|A_{i,j}(\Lambda - \sigma_s I)\|_{B(\ell^1_\nu, \ell^1_\nu)}, \qquad \alpha_{i,j}^{(2)} \stackrel{\text{def}}{=} \|A_{i,j}\Lambda\|_{B(\ell^1_\nu, \ell^1_\nu)},
\end{aligned}$$

so that

$$\|AD_x^2 f(w, \sigma_s)(u,v)\|_{\mathbb{X}} \le \max_{i=1,2,3} \left(\hat{\alpha}_{i,2}(w) + \hat{\alpha}_{i,3}(w)\right).$$

To compute the bounds $\alpha_{i,j}^{(k)}$ $(i, j = 2, 3,\ k = 1, 2)$, we use formula (41). For $\alpha_{i,j}^{(1)}$ we use interval arithmetic and replace σ_s by the interval $[\sigma_0, \sigma_1]$, and rigorously obtain

the bound. Moreover,

$$\begin{aligned}(D_{x,\sigma}f(\bar{x}_0,\sigma_t)v)_1 &= 0\\ (D_{x,\sigma}f(\bar{x}_0,\sigma_t)v)_2 &= D_{x,\sigma}g(\bar{x}_0,\sigma_t)v = -\lambda^v\bar{a}_0 - \bar{\lambda}_0 a^v\\ (D_{x,\sigma}f(\bar{x}_0,\sigma_t)v)_3 &= D_{x,\sigma}h(\bar{x}_0,\sigma_t)v = -\lambda^v\bar{b}_0 - \bar{\lambda}_0 b^v.\end{aligned}$$

Hence, for $i = 1,2,3$,

$$\begin{aligned}\|A_{i,2}D_{x,\sigma}g(\bar{x}_0,\sigma_t)v\|^{(i)} &\leq \hat{\beta}_{i,2} \stackrel{\text{def}}{=} \beta_{i,2}\left(\|\bar{a}_0\|_{1,\nu} + |\bar{\lambda}_0|\right)\\ \|A_{i,3}D_{x,\sigma}h(\bar{x}_0,\sigma_t)v\|^{(i)} &\leq \hat{\beta}_{i,3} \stackrel{\text{def}}{=} \beta_{i,3}\left(\|\bar{b}_0\|_{1,\nu} + |\bar{\lambda}_0|\right),\end{aligned}$$

where

$$\beta_{1,j} \stackrel{\text{def}}{=} \|A_{1,j}\|_{\infty,\nu^{-1}} \quad \text{and} \quad \beta_{i,j} \stackrel{\text{def}}{=} \|A_{i,j}\|_{B(\ell^1_\nu,\ell^1_\nu)} \quad \text{for } j = 2,3.$$

Define

$$\hat{a} \stackrel{\text{def}}{=} \sup_{s\in[0,1]} \|\bar{a}_s\|_{1,\nu}, \quad \hat{b} \stackrel{\text{def}}{=} \sup_{s\in[0,1]} \|\bar{b}_s\|_{1,\nu}, \quad \hat{\lambda} \stackrel{\text{def}}{=} \sup_{s\in[0,1]} |\bar{\lambda}_s|$$

and assuming that $r \leq r_*$, we can conclude that

$$\begin{aligned}\sup_{\substack{w\in B_r(\bar{x}_s)\\ u,v\in B_1(0)\\ s\in[0,1]}} \|AD_x^2 f(w,\sigma_s)(u,v)\|_{\mathbb{X}} &\leq \sup_{w\in B_r(\bar{x}_s)} \max_{i=1,2,3}\left(\hat{\alpha}_{i,2}(w) + \hat{\alpha}_{i,3}(w)\right)\\ &\leq Z_2^{(2)} \stackrel{\text{def}}{=} \max\left(\frac{1}{\delta}Z_{2,1}^{(2)}, Z_{2,2}^{(2)}, Z_{2,3}^{(2)}\right),\end{aligned}$$

where

$$\begin{aligned}Z_{2,i}^{(2)} \stackrel{\text{def}}{=}\ & 2\delta\alpha_{i,2}^{(1)} + 6\alpha_{i,2}^{(2)}(\hat{a}+r_*)(\delta\hat{a}+\hat{\lambda}+2\delta r_*) + 2\delta\alpha_{i,3}^{(1)}\\ &+ 3\alpha_{i,3}^{(2)}\left(4\delta(\hat{a}+r_*)(\hat{b}+r_*) + 2\delta(\hat{a}+r_*)^2 + 2(\hat{\lambda}+\delta r_*)(2\hat{a}+\hat{b}+3r_*)\right).\end{aligned}$$

Moreover,

$$\begin{aligned}&\sup_{\substack{s,t\in[0,1]\\ u,v\in B_1(0)}} \|AD_x^2 f(\bar{x}_t,\sigma_s)(u,v)\|_{\mathbb{X}}\|\bar{x}_1 - \bar{x}_0\|_{\mathbb{X}}\\ &\qquad \leq Z_2^{(1)} \stackrel{\text{def}}{=} \max\left(\frac{1}{\delta}Z_{2,1}^{(1)}, Z_{2,2}^{(1)}, Z_{2,3}^{(1)}\right)\|\bar{x}_1 - \bar{x}_0\|_{\mathbb{X}},\end{aligned}$$

where

$$Z_{2,i}^{(1)} \stackrel{\text{def}}{=} 2\delta\alpha_{i,2}^{(1)} + 6\alpha_{i,2}^{(2)}\hat{a}(\delta\hat{a}+\hat{\lambda}) + 2\delta\alpha_{i,3}^{(1)} + 3\alpha_{i,3}^{(2)}\left(4\delta\hat{a}\hat{b} + 2\delta\hat{a}^2 + 2\hat{\lambda}(2\hat{a}+\hat{b})\right).$$

Setting

$$Z_2^{(0)} \stackrel{\text{def}}{=} \max\left(\frac{1}{\delta}\left(\hat{\beta}_{1,2}+\hat{\beta}_{1,3}\right),\ \hat{\beta}_{2,2}+\hat{\beta}_{2,3}\ , \hat{\beta}_{3,2}+\hat{\beta}_{3,3}\right)|\sigma_1 - \sigma_0|,$$

we let

$$Z_2(r) \stackrel{\text{def}}{=} Z_2^{(2)}r + Z_2^{(1)} + Z_2^{(0)}, \tag{65}$$

which is by construction a bound satisfying (54).

Combining (57), (58), (63) and (65) leads to the radii polynomial

$$\begin{aligned}p(r) &\stackrel{\text{def}}{=} Z_2(r)r - (1 - Z_0 - Z_1)r + Y_0 \qquad (66)\\ &= Z_2^{(2)}r^2 - (1 - Z_0 - Z_1 - Z_2^{(1)} - Z_2^{(0)})r + Y_0.\end{aligned}$$

Recall that the radii polynomial approach consists of applying Theorem 3.5, that is to find a radius $r_0 > 0$ such that the radii polynomial (66) satisfies $p(r_0) < 0$.

This implies the existence of a C^∞ function $\tilde{x} : [0,1] \to \bigcup_{s\in[0,1]} B_{r_0}(\bar{x}_s)$ such that $f(\tilde{x}(s), \sigma_s) = 0$, for all $s \in [0,1]$. Using the radii polynomial (66), we present in Section 3.5.1 computer-assisted proofs providing existence of three smooth global branches of saddle-node bifurcations in the (σ, λ) parameter space.

3.4. **The radii polynomial for pitchfork bifurcations.** We consider two symmetries S_1, S_2 given by

$$(S_1 u)(y) \overset{\text{def}}{=} -u(1-y) \qquad \text{and} \qquad (S_2 u)(y) \overset{\text{def}}{=} u(1-y) \tag{67}$$

and for $i = 1, 2$, define

$$X_s^{(i)} = \{u \in X \ : \ S_i u = u\} \qquad \text{and} \qquad X_a^{(i)} = \{v \in X \ : \ S_i v = -v\}.$$

The corresponding Banach spaces in Fourier space are given by

$$X_s^{(1)} = \left\{a = (a_k)_{k\geq 1} \in \ell^1_\nu \ : \ a_{2j} = 0, \text{ for all } j \geq 1\right\}$$
$$X_a^{(1)} = \left\{b = (b_k)_{k\geq 1} \in \ell^1_\nu \ : \ b_{2j-1} = 0, \text{ for all } j \geq 1\right\}$$

and

$$X_s^{(2)} = \left\{a = (a_k)_{k\geq 1} \in \ell^1_\nu \ : \ a_{2j-1} = 0, \text{ for all } j \geq 1\right\}$$
$$X_a^{(2)} = \left\{b = (b_k)_{k\geq 1} \in \ell^1_\nu \ : \ b_{2j} = 0, \text{ for all } j \geq 1\right\}.$$

Given $i \in \{1, 2\}$, define the Banach space

$$\mathbb{X}^{(i)} = \mathbb{R} \times X_s^{(i)} \times \ell^1_\nu$$

endowed, given a weight $\delta > 0$, with the weighed norm

$$\|x\|_{\mathbb{X}^{(i)}} = \max\left(\frac{1}{\delta}|\lambda|, \|a\|^{(i)}_{1,\nu}, \|b\|_{1,\nu}\right), \tag{68}$$

where

$$\|a\|^{(i)}_{1,\nu} = 2\sum_{k\geq 1} |a_k|\nu^k = \begin{cases} 2\displaystyle\sum_{j\geq 1} |a_{2j-1}|\nu^{2j-1}, & i = 1 \\ 2\displaystyle\sum_{j\geq 1} |a_{2j}|\nu^{2j}, & i = 2. \end{cases}$$

Recall that for $k \geq 1$,

$$\mu_k(\lambda) \overset{\text{def}}{=} -k^4\pi^4 + \lambda k^2\pi^2 - \lambda\sigma$$

and recalling from (27) and from (30),

$$g_k(\lambda, a) = \mu_k(\lambda)a_k - \lambda k^2\pi^2(a^3)_k$$
$$h_k(\lambda, a, b) = \mu_k(\lambda)b_k - 3\lambda k^2\pi^2(a^2 b)_k.$$

Let $x = (\lambda, a, b) \in \mathbb{R} \times X_s^{(i)} \times \ell^1_\nu$, then define f_r by

$$f_r(x) = \begin{pmatrix} \eta(b) \\ g(\lambda, a) \\ h(\lambda, a, b) \end{pmatrix}, \tag{69}$$

where $\eta(b) = \frac{1}{\bar{b}_{k_0}} b_{k_0} - 1$, that is $\eta(b) = 0$ implies that the k_0-th component of the eigenvector b equals the fixed value $\bar{b}_{k_0}$.

Given $a \in X_s^{(1)}$, that is $a = (a_k)_{k\geq 1}$ such that $a_{2j} = 0$ for all $j \geq 1$, then

$$\begin{aligned} g_{2j}(\lambda, a) &= \mu_{2j}(\lambda)a_{2j} - \lambda(2j)^2\pi^2(a^3)_{2j} \\ &= \mu_{2j}(\lambda)a_{2j} - \lambda(2j)^2\pi^2 \sum_{\substack{k_1+k_2+k_3=2j \\ k_i\in\mathbb{Z}\setminus\{0\}}} a_{|k_1|}a_{|k_2|}a_{|k_3|} = 0, \end{aligned}$$

since for any $(k_1, k_2, k_3) \in (\mathbb{Z} \setminus \{0\})^3$, the relation $k_1 + k_2 + k_3 = 2j$ implies that there must be $i \in \{1, 2, 3\}$ such that k_i is even, and so $a_{|k_i|} = 0$.

Similarly, given $a \in X_s^{(2)}$, that is $a = (a_k)_{k\geq 1}$ such that $a_{2j-1} = 0$ for all $j \geq 1$, then

$$\begin{aligned} g_{2j-1}(\lambda, a) &= \mu_{2j-1}(\lambda)a_{2j-1} - \lambda(2j-1)^2\pi^2(a^3)_{2j-1} \\ &= \mu_{2j-1}(\lambda)a_{2j-1} - \lambda(2j-1)^2\pi^2 \sum_{\substack{k_1+k_2+k_3=2j-1 \\ k_i\in\mathbb{Z}\setminus\{0\}}} a_{|k_1|}a_{|k_2|}a_{|k_3|} = 0, \end{aligned}$$

since for any $(k_1, k_2, k_3) \in (\mathbb{Z} \setminus \{0\})^3$, the relation $k_1 + k_2 + k_3 = 2j - 1$ implies that there must be $i \in \{1, 2, 3\}$ such that k_i is odd, and so $a_{|k_i|} = 0$.

To verify rigorously a pitchfork bifurcation, we use the general approach of Section 3.2, as in the case of saddle-node bifurcations. All estimates are similar as in the case of saddle-node bifurcations, expect that in this case we consider the norm $\|\cdot\|_{\mathbb{X}^{(i)}}$ given in (68), where the index i depends on the *symmetry* of the bifurcation. This implies that all expansions are the same, but the norms are replaced by (68). Using these new expansions, we define the equivalent radii polynomial

$$p(r) = Z_2^{(2)}r^2 - (1 - Z_0 - Z_1 - Z_2^{(1)} - Z_2^{(0)})r + Y_0, \tag{70}$$

which is the same as the one defined in (66), except that the bounds $Z_0, Z_1, Z_2^{(0)}, Z_2^{(1)}$ and $Z_2^{(2)}$ defining it are slightly different, as they come from a different problem.

3.5. **Results.** In this section, we are finally ready to state our results, which consist of a set of three validated branches of saddle-node bifurcations and three validated branches of symmetry-breaking pitchfork bifurcations. As mentioned in the introduction, each of these cases were found numerically in [17], where it was observed numerically that there was a common scaling law for different bifurcation branches. The choice of bifurcation points was made in a somewhat arbitrary way as secondary bifurcation point for small λ that still satisfied the conditions of our theorem. We emphasize that the validation of these branches of bifurcations serves two purposes: first, they illustrate our general functional analytic methods, methods which can easily be adapted to other equations. Second, for the diblock copolymer equation, this is a first step towards our eventual goal of validating the scalings of branches that we have observed in the previous paper. We state each of these results as a theorem, which is presented along with an associated table giving the detailed information on the Fourier coefficients found for each solution. The tables are presented for completeness and preciseness, but we do not expect that a reader would find the data particularly illuminating unless it was being used as a basis for future work.

For all the computer-assisted proofs, the weight δ in the definition the norm of the Banach spaces is fixed to be equal to the numerical value $\bar{\lambda}_0$. This choice of weight δ is used to compensate for the fact that the variable λ sometimes is several orders of magnitude larger than the $\|a\|_{1,\nu}$ and $\|b\|_{1,\nu}$. All proofs are performed

using MATLAB codes available at [21] and use the interval arithmetic package INTLAB [30].

3.5.1. *Saddle-Node Bifurcation Points.* We begin by presenting three sample theorems of existence of saddle-node bifurcations at the fixed parameter value $\sigma = 6$, which we proved using the radii polynomial (66) and Theorem 3.5. Note that the direction of the bifurcation (i.e. the sign of ϱ in Proposition 2.11) was not important for our purposes, so we did not compute it. In order to do so, we would have to validate the sign of the involved reals, which would not be hard, but would involve a norm bound for the involved derivatives.

Theorem 3.7. *At $\sigma_0 = 6$, the nonlinear diblock-copolymer equation (1) undergoes a saddle-node bifurcation at a point $(\tilde\lambda_0, \tilde u_0)$, where $\tilde\lambda_0 \in \bar\lambda_0 \pm r[-1,1]$ with $\bar\lambda_0 = 262.9276507797089$ and $r = 1.1 \times 10^{-10}$. The point $\tilde u_0$ is given by $\tilde u_0(y) = 2\sum_{k\geq 1} \tilde a_k \cos(k\pi y)$, with $\|\tilde a - \bar a\|_{1,\nu} \leq r$, where the Fourier coefficients of $\bar a$ are given in Table 9. Moreover, $\|\tilde u_0 - \bar u_0\|_{C^0} \leq 1.1\times 10^{-10}$, where $\bar u_0(y) = 2\sum_{k\geq 1} \bar a_k \cos(k\pi y)$.*

The saddle-node bifurcation point of Theorem 3.7 is portrayed in Figure 3.

Proof. Fix $\nu = 1.01$ and $m = 48$. The Fourier coefficients associated to the numerical approximation $\bar x_0 \in \mathbb{R}^{2m-1} = \mathbb{R}^{95}$ are given in the MATLAB datafile `pt0_sn.mat`. The MATLAB script `script_proof_sn_pt0.m` computes the coefficients of the radii polynomials and verifies that for $r = 1.1 \times 10^{-10}$, the radii polynomial satisfies defined in (55) $p(r) < 0$. Therefore by Theorem 3.5, there exists a unique $\tilde x = (\tilde\lambda_0, \tilde a, \tilde b) \in B_r(\bar x_0) \subset \mathbb{X}$ such that $f(\tilde x) = 0$ where f is given in (31). The solution $\tilde x$ corresponds to an isolated non-degenerate zero $(\tilde\lambda_0, \tilde u_0, \tilde v_0)$ solving the equation $\mathcal{F}(\lambda, u, v) = (0,0,0)$. By Proposition 2.15, Theorem 2.10 and Proposition 2.9, it follows that (1) undergoes a saddle-node bifurcation at $(\tilde\lambda_0, \tilde u_0)$. □

Theorem 3.8. *At $\sigma_0 = 6$, the nonlinear diblock-copolymer equation (1) undergoes a saddle-node bifurcation at a point $(\tilde\lambda_0, \tilde u_0)$, where $\tilde\lambda_0 \in \bar\lambda_0 \pm r[-1,1]$ with $\bar\lambda_0 = 681.3850215638124$ and $r = 6.2 \times 10^{-13}$. The point $\tilde u_0$ is given by $\tilde u_0(y) = 2\sum_{k\geq 1} \tilde a_k \cos(k\pi y)$, with $\|\tilde a - \bar a\|_{1,\nu} \leq r$, where the Fourier coefficients of $\bar a$ are given in Table 10. Moreover, $\|\tilde u_0 - \bar u_0\|_{C^0} \leq 6.2\times 10^{-13}$, where $\bar u_0(y) = 2\sum_{k\geq 1} \bar a_k \cos(k\pi y)$.*

The saddle-node bifurcation point of Theorem 3.8 is portrayed in the left part of Figure 6.

Proof. The proof is similar to the proof of Theorem 3.7. In this case $\nu = 1.01$, $m = 89$, and the MATLAB script `script_proof_sn_pt1.m` computes the coefficients of the radii polynomials with interval arithmetic and the Fourier coefficients associated to the numerical approximation $\bar x_0 \in \mathbb{R}^{2m-1} = \mathbb{R}^{177}$ are given in the MATLAB datafile `pt1_sn.mat`. □

Theorem 3.9. *At $\sigma_0 = 6$, the nonlinear diblock-copolymer equation (1) undergoes a saddle-node bifurcation at a point $(\tilde\lambda_0, \tilde u_0)$, where $\tilde\lambda_0 \in \bar\lambda_0 \pm r[-1,1]$ with $\bar\lambda_0 = 1343.284789160779$ and $r = 1.1 \times 10^{-12}$. The point $\tilde u_0$ is given by $\tilde u_0(y) = 2\sum_{k\geq 1} \tilde a_k \cos(k\pi y)$, with $\|\tilde a - \bar a\|_{1,\nu} \leq r$. Moreover, $\|\tilde u_0 - \bar u_0\|_{C^0} \leq 1.1 \times 10^{-12}$, where $\bar u_0(y) = 2\sum_{k\geq 1} \bar a_k \cos(k\pi y)$.*

The saddle-node bifurcation point of Theorem 3.9 is portrayed in the right part of Figure 6.

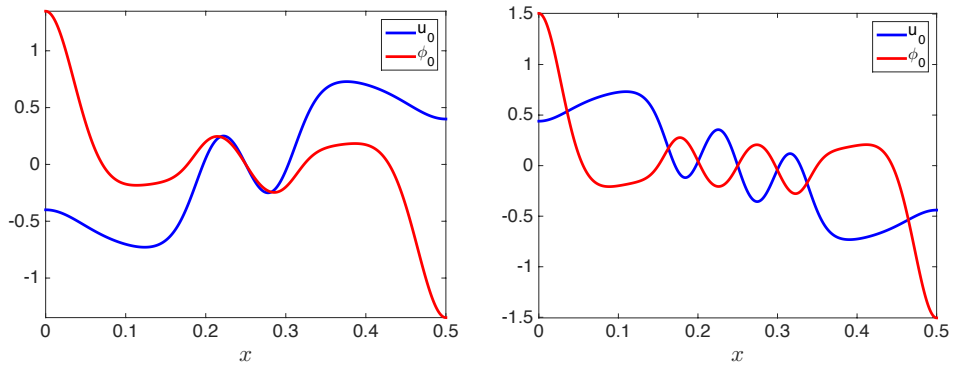

FIGURE 6. Equilibrium solutions u_0 (in blue) of the diblock copolymer equation for $\sigma_0 = 6$, together with their associated kernel functions (in red). On left $\lambda_0 \approx 681.4$, on right $\lambda_0 \approx 1343.3$. These two distinct stationary solutions are both saddle-node bifurcation points. The equilibrium on the left (respectively right) is rigorously proved in Theorem 3.8 (respectively Theorem 3.9).

Proof. The proof is similar to the proof of Theorem 3.7. In this case $\nu = 1.01$, $m = 121$, and the MATLAB script `script_proof_sn_pt2.m` computes the coefficients of the radii polynomials with interval arithmetic and the Fourier coefficients associated to the numerical approximation $\bar{x}_0 \in \mathbb{R}^{2m-1} = \mathbb{R}^{241}$ are given in the MATLAB datafile `pt2_sn.mat`. □

Using the radii polynomial approach, we proved the following three results.

Theorem 3.10. *There is a branch of saddle-node bifurcations parameterized by the parameter $\sigma \in [4.6762, 8.8812]$. The global branch contains the point of Theorem 3.7 and is a C^∞ function of the parameter σ. The continuous range of parameter λ of the saddle-node bifurcations over the branch contains the interval $\lambda \in [98.72, 1808.99]$.*

The branch of saddle-node bifurcations proven in Theorem 3.10 is portrayed in red in Figure 7.

Theorem 3.11. *There is a branch of saddle-node bifurcations parameterized by the parameter $\sigma \in [4.8634, 9.4444]$. The global branch contains the point of Theorem 3.8 and is a C^∞ function of the parameter σ. The continuous range of parameter λ of the saddle-node bifurcations over the branch contains the interval $\lambda \in [259.18, 2264.67]$.*

The branch of saddle-node bifurcations proven in Theorem 3.11 is portrayed in green in Figure 7.

Theorem 3.12. *There is a branch of saddle-node bifurcations parameterized by the parameter $\sigma \in [5.2595, 9.5322]$. The global branch contains the point of Theorem 3.9 and is a C^∞ function of the parameter σ. The continuous range of parameter λ of the saddle-node bifurcations over the branch contains the interval $\lambda \in [508.539, 2360.55]$.*

The branch of saddle-node bifurcations proven in Theorem 3.12 is portrayed in blue in Figure 7.

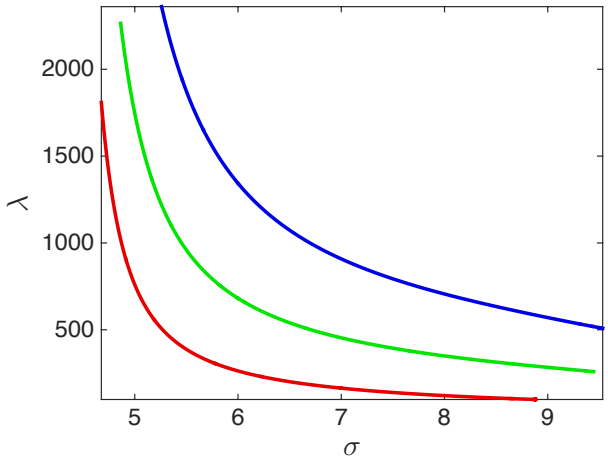

FIGURE 7. Three global C^∞ branches of saddle-node bifurcation points of the diblock copolymer equation. The red (respectively green, blue) branch is proven in Theorem 3.10 (respectively Theorem 3.11, Theorem 3.12).

3.5.2. *Pitchfork Bifurcation Points.* We begin by presenting three theorems of existence of pitchfork bifurcations at the fixed parameter value $\sigma = 6$, which we proved using the radii polynomial (70) together with Theorem 3.5.

Theorem 3.13. *At $\sigma_0 = 6$, the nonlinear diblock-copolymer equation (1) undergoes a pitchfork bifurcation at a point $(\tilde\lambda_0, \tilde u_0)$, breaking the symmetry S_1 defined in (67), where $\tilde\lambda_0 \in \bar\lambda_0 \pm r[-1,1]$ with $\bar\lambda_0 = 142.0626439889047$ and $r = 2.37 \times 10^{-11}$. The point $\tilde u_0$ is given by the expansion $\tilde u_0(y) = 2\sum_{j\geq 1} \tilde a_{2j-1}\cos((2j-1)\pi y)$ with $\|\tilde a - \bar a\|_{1,\nu} \leq r$, where the Fourier coefficients of $\bar a$ are given in Table 11. Moreover, $\|\tilde u_0 - \bar u_0\|_{C^0} \leq 2.37 \times 10^{-11}$, where $\bar u_0(y) = 2\sum_{j\geq 1} \bar a_{2j-1}\cos((2j-1)\pi y)$.*

The bifurcation point of Theorem 3.13 is portrayed in the top left plot of Figure 4.

Proof. Fix $\nu = 1.01$ and $m = 46$. The Fourier coefficients associated to the numerical approximation $\bar x_0 \in \mathbb{R}^{3m/2} = \mathbb{R}^{69}$ are given in the MATLAB datafile `pt_032.mat`. The MATLAB script `proof_thm1_pitchfork.m` computes the coefficients of the radii polynomials and verifies that for $r = 2.37 \times 10^{-11}$, the radii polynomial satisfies defined in (55) $p(r) < 0$. Therefore by Theorem 3.5, there exists a unique $\tilde x = (\tilde\lambda_0, \tilde a, \tilde b) \in B_r(\bar x_0) \subset \mathbb{X}^{(1)}$ such that $f_r(\tilde x) = 0$ where f_r is given in (69). The solution $\tilde x$ corresponds to an isolated non-degenerate zero $(\tilde\lambda_0, \tilde u_0, \tilde\varphi_0)$ solving the equation $\mathcal{F}_r(\lambda, u, \varphi) = (0,0,0)$. By Proposition 2.15, Theorem 2.12 and Proposition 2.11, it follows that (1) undergoes a pitchfork bifurcation at $(\tilde\lambda_0, \tilde u_0)$. □

Theorem 3.14. *At $\sigma_0 = 6$, the nonlinear diblock-copolymer equation (1) undergoes a pitchfork bifurcation at a point $(\tilde\lambda_0, \tilde u_0)$, breaking the symmetry S_2 defined in (67), where $\tilde\lambda_0 \in \bar\lambda_0 \pm r[-1,1]$ with $\bar\lambda_0 = 53.58536646961630$ and $r = 3.28 \times 10^{-13}$. The point $\tilde u_0$ is given by the expansion $\tilde u_0(y) = 2\sum_{j\geq 1} \tilde a_{2j}\cos(2j\pi y)$ with $\|\tilde a - \bar a\|_{1,\nu} \leq r$, where the Fourier coefficients of $\bar a$ are given in Table 12. Moreover, $\|\tilde u_0 - \bar u_0\|_{C^0} \leq 3.28 \times 10^{-13}$, where $\bar u_0(y) = 2\sum_{j\geq 1} \bar a_{2j}\cos(2j\pi y)$.*

The bifurcation point of Theorem 3.14 is portrayed in the top right plot of Figure 4.

Proof. The proof is similar to the proof of Theorem 3.13. In this case $\nu = 1.1$, $m = 29$, and the MATLAB script `proof_thm2_pitchfork.m` computes the coefficients of the radii polynomials with interval arithmetic and the Fourier coefficients associated to the numerical approximation $\bar{x}_0 \in \mathbb{R}^{3(m-1)/2} = \mathbb{R}^{43}$ are given in the MATLAB datafile `pt_105.mat`. □

Theorem 3.15. *At $\sigma_0 = 6$, the nonlinear diblock-copolymer equation (1) undergoes a pitchfork bifurcation at a point $(\tilde{\lambda}_0, \tilde{u}_0)$, breaking the symmetry S_2 defined in (67), where $\tilde{\lambda}_0 \in \bar{\lambda}_0 \pm r[-1,1]$ with $\bar{\lambda}_0 = 203.0932198783432$ and $r = 1.88 \times 10^{-12}$. The point $\tilde{u}_0$ is given by the expansion $\tilde{u}_0(y) = 2\sum_{j\geq 1} \tilde{a}_{2j} \cos(2j\pi y)$ with $\|\tilde{a} - \bar{a}\|_{1,\nu} \leq r$, where the Fourier coefficients of $\bar{a}$ are given in Table 13. Moreover, $\|\tilde{u}_0 - \bar{u}_0\|_{C^0} \leq 1.88 \times 10^{-12}$, where $\bar{u}_0(y) = 2\sum_{j\geq 1} \bar{a}_{2j} \cos(2j\pi y)$.*

The bifurcation point of Theorem 3.15 is portrayed in the bottom right plot of Figure 4.

Proof. The proof is similar to the proof of Theorem 3.13. In this case $\nu = 1.01$, $m = 57$, and the MATLAB script `proof_thm3_pitchfork.m` computes the coefficients of the radii polynomials with interval arithmetic and the Fourier coefficients associated to the numerical approximation $\bar{x}_0 \in \mathbb{R}^{3(m-1)/2} = \mathbb{R}^{85}$ are given in the MATLAB datafile `pt_174.mat`. □

In the last three theorems, we have established the existence of pitchfork bifurcation points. The next three theorems establish that each of these points lies within a branch in the two-parameter $\lambda - \sigma$-plane.

Theorem 3.16. *There is a branch of pitchfork bifurcations (breaking the symmetry S_1) parameterized by the parameter $\sigma \in [4.98384, 7.8852]$. The global branch contains the point of Theorem 3.13 and is a C^∞ function of the parameter σ. The continuous range of parameter λ of the pitchfork bifurcations over the branch contains the interval $\lambda \in [49.5782, 456]$.*

The branch of pitchfork bifurcations of Theorem 3.16 is portrayed in red in Figure 8.

Theorem 3.17. *There is a branch of pitchfork bifurcations (breaking the symmetry S_2) parameterized by the parameter $\sigma \in [0.04618, 7.813]$. The global branch contains the point of Theorem 3.14 and is a C^∞ function of the parameter σ. The continuous range of parameter λ of the pitchfork bifurcations over the branch contains the interval $\lambda \in [49.497, 210.735]$.*

The branch of pitchfork bifurcations of Theorem 3.17 is portrayed in green in Figure 8.

Theorem 3.18. *There is a branch of pitchfork bifurcations (breaking the symmetry S_2) parameterized by the parameter $\sigma \in [0.8353, 9.28807]$. The global branch contains the point of Theorem 3.15 and is a C^∞ function of the parameter σ. The continuous range of parameter λ of the pitchfork bifurcations over the branch contains the interval $\lambda \in [167.791, 415.757]$.*

The branch of pitchfork bifurcations of Theorem 3.18 is portrayed in blue in Figure 8.

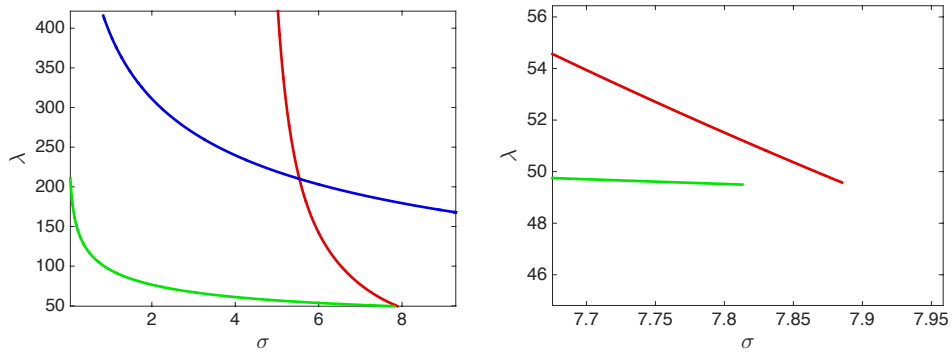

FIGURE 8. (Left) Global C^∞ branches of pitchfork bifurcations points of the nonlinear diblock-copolymer equation (1). The red (respectively green, blue) branch is proven in Theorem 3.16 (respectively Theorem 3.17, Theorem 3.18). (Right) Zoom-in of the branches.

k	$\bar{a}_k$
1	$3.425518079006526 \times 10^{-01}$
3	$-1.974141656767766 \times 10^{-01}$
5	$3.282914954203388 \times 10^{-02}$
7	$-2.113767170849276 \times 10^{-02}$
9	$6.009282870770884 \times 10^{-03}$
11	$-2.511019989454085 \times 10^{-03}$
13	$9.094914470604478 \times 10^{-04}$
15	$-3.384556275954580 \times 10^{-04}$
17	$1.276639504135262 \times 10^{-04}$
19	$-4.725661956005324 \times 10^{-05}$
21	$1.774095811379435 \times 10^{-05}$
23	$-6.609023152112926 \times 10^{-06}$
25	$2.470638409851695 \times 10^{-06}$
27	$-9.226037848187633 \times 10^{-07}$
29	$3.445645075514765 \times 10^{-07}$
31	$-1.287116825741538 \times 10^{-07}$
33	$4.807038316262538 \times 10^{-08}$
35	$-1.795559964584755 \times 10^{-08}$
37	$6.706444497377878 \times 10^{-09}$
39	$-2.504938910570366 \times 10^{-09}$
41	$9.356049310264420 \times 10^{-10}$
43	$-3.494257722696195 \times 10^{-10}$
45	$1.304418365890033 \times 10^{-10}$
47	$-4.874587773792928 \times 10^{-11}$
≥ 48	0

FIGURE 9. The cosine Fourier coefficients of the saddle-node bifurcation point from Theorem 3.7. We show $\bar{a}_k$ for $k \geq 1$. Note that all even coefficients are 0.

Acknowledgments. This research was supported in part by the Institute for Mathematics and its Applications at the University of Minnesota with funds provided by the National Science Foundation. In addition, this work was partially supported by NSF grants DMS-0907818, DMS-1114923, and DMS-1407087.

k	$\bar{a}_k$
1	$-3.322748897308590 \times 10^{-01}$
3	$5.964807310189380 \times 10^{-02}$
5	$1.098656423542226 \times 10^{-01}$
7	$-7.147163509374215 \times 10^{-02}$
9	$4.621259346913079 \times 10^{-02}$
11	$-1.499847066658469 \times 10^{-02}$
13	$2.771825017383096 \times 10^{-03}$
15	$1.361700989591935 \times 10^{-03}$
17	$-1.209183257116878 \times 10^{-03}$
19	$4.001695298106526 \times 10^{-04}$
21	$1.012053583674478 \times 10^{-04}$
23	$-2.188388273353959 \times 10^{-04}$
25	$1.583392405367557 \times 10^{-04}$
27	$-7.312323758516202 \times 10^{-05}$
29	$1.946946540531770 \times 10^{-05}$
31	$1.490247191381953 \times 10^{-06}$
33	$-4.856412723117526 \times 10^{-06}$
35	$2.675779467405178 \times 10^{-06}$
37	$-4.983777798680973 \times 10^{-07}$
39	$-4.341948283537669 \times 10^{-07}$
41	$5.122942462431431 \times 10^{-07}$
43	$-3.029210231609401 \times 10^{-07}$
45	$1.114997949387757 \times 10^{-07}$
47	$-1.399986292600402 \times 10^{-08}$
49	$-1.413350705303663 \times 10^{-08}$
51	$1.234615338731550 \times 10^{-08}$
53	$-4.811188646022121 \times 10^{-09}$
55	$7.635825922534573 \times 10^{-11}$
57	$1.346542437697546 \times 10^{-09}$
59	$-1.114761302006941 \times 10^{-09}$
61	$5.360571766016584 \times 10^{-10}$
63	$-1.403428779571979 \times 10^{-10}$
65	$-1.984767195915526 \times 10^{-11}$
67	$4.496258857946458 \times 10^{-11}$
69	$-2.598922926741918 \times 10^{-11}$
71	$6.827356566319794 \times 10^{-12}$
73	$2.040570417154504 \times 10^{-12}$
75	$-3.518846286971038 \times 10^{-12}$
77	$2.242152802281248 \times 10^{-12}$
79	$-8.494640661551343 \times 10^{-13}$
81	$1.000445609992326 \times 10^{-13}$
83	$1.237989407717937 \times 10^{-13}$
85	$-1.097953126715571 \times 10^{-13}$
87	$4.696530654231161 \times 10^{-14}$
≥ 88	0

FIGURE 10. The cosine Fourier coefficients of the saddle-node bifurcation point from Theorem 3.8. We show $\bar{a}_k$ for $k \geq 1$. Note that all even coefficients are 0.

k	$\bar{a}_k$
1	$3.543753443245022 \times 10^{-01}$
3	$-1.006781087499776 \times 10^{-01}$
5	$1.774717239183692 \times 10^{-02}$
7	$-4.253838897909598 \times 10^{-03}$
9	$9.487830638572718 \times 10^{-04}$
11	$-2.154147796091226 \times 10^{-04}$
13	$4.890289353907032 \times 10^{-05}$
15	$-1.110225418059996 \times 10^{-05}$
17	$2.521609074712272 \times 10^{-06}$
19	$-5.727445161875873 \times 10^{-07}$
21	$1.300994133620561 \times 10^{-07}$
23	$-2.955313733270058 \times 10^{-08}$
25	$6.713369627113701 \times 10^{-09}$
27	$-1.525046630395195 \times 10^{-09}$
29	$3.464409773915803 \times 10^{-10}$
31	$-7.870055534981058 \times 10^{-11}$
33	$1.787837280778145 \times 10^{-11}$
35	$-4.061433389832354 \times 10^{-12}$
37	$9.226383862676367 \times 10^{-13}$
39	$-2.095966548542377 \times 10^{-13}$
41	$4.761431600794773 \times 10^{-14}$
43	$-1.081662061453402 \times 10^{-14}$
45	$2.457248823477995 \times 10^{-15}$
≥ 46	0

FIGURE 11. The cosine Fourier coefficients of the pitchfork bifurcation point from Theorem 3.13. We show $\bar{a}_k$ for $k \geq 1$. Note that all even coefficients are 0.

k	$\bar{a}_k$
2	$1.932032148778461 \times 10^{-01}$
6	$-1.228415125053532 \times 10^{-03}$
10	$7.745221377996015 \times 10^{-06}$
14	$-4.899802649253310 \times 10^{-08}$
18	$3.101012396194486 \times 10^{-10}$
22	$-1.962774847496414 \times 10^{-12}$
26	$1.242372383052349 \times 10^{-14}$
≥ 27	0

FIGURE 12. The cosine Fourier coefficients of the pitchfork bifurcation point from Theorem 3.14. We show $\bar{a}_k$ for $k \geq 2$. Note that all other coefficients are 0.

k	$\bar{a}_k$
4	$2.491592573155594 \times 10^{-01}$
12	$-2.427167305846578 \times 10^{-03}$
20	$2.379666082383739 \times 10^{-05}$
28	$-2.334882400787356 \times 10^{-07}$
36	$2.291173981628420 \times 10^{-09}$
44	$-2.248336688870471 \times 10^{-11}$
52	$2.206286704017840 \times 10^{-13}$
≥ 53	0

FIGURE 13. The cosine Fourier coefficients of the pitchfork bifurcation point from Theorem 3.15. We show $\bar{a}_k$ for $k \geq 2$. Note that all other coefficients are 0.

REFERENCES

[1] G. Arioli and H. Koch, Computer-assisted methods for the study of stationary solutions in dissipative systems, applied to the Kuramoto-Sivashinski equation, *Arch. Ration. Mech. Anal.*, **197** (2010), 1033–1051.

[2] G. Arioli and H. Koch, Integration of dissipative partial differential equations: A case study, *SIAM Journal on Applied Dynamical Systems*, **9** (2010), 1119–1133.

[3] M. Bahiana and Y. Oono, Cell dynamical system approach to block copolymers, *Physical Review A*, **41** (1990), 6763–6771.

[4] D. Blömker, B. Gawron and T. Wanner, Nucleation in the one-dimensional stochastic Cahn-Hilliard model, *Discrete and Continuous Dynamical Systems, Series A*, **27** (2010), 25–52.

[5] D. Blömker, S. Maier-Paape and T. Wanner, Phase separation in stochastic Cahn-Hilliard models, in *Mathematical Methods and Models in Phase Transitions* (ed. A. Miranville), Nova Science Publishers, New York, 2005, 1–41.

[6] D. Blömker, E. Sander and T. Wanner, Degenerate nucleation in the Cahn-Hilliard-Cook model, *SIAM Journal on Applied Dynamical Systems*, **15** (2016), 459–494.

[7] M. Breden, J.-P. Lessard and M. Vanicat, Global bifurcation diagrams of steady states of systems of PDEs via rigorous numerics: A 3-component reaction-diffusion system, *Acta Appl. Math.*, **128** (2013), 113–152.

[8] R. Choksi, M. A. Peletier and J. F. Williams, On the phase diagram for microphase separation of diblock copolymers: An approach via a nonlocal Cahn-Hilliard functional, *SIAM Journal on Applied Mathematics*, **69** (2009), 1712–1738.

[9] R. Choksi and X. Ren, On the derivation of a density functional theory for microphase separation of diblock copolymers, *Journal of Statistical Physics*, **113** (2003), 151–176.

[10] P. Chossat and R. Lauterbach, *Methods in Equivariant Bifurcations and Dynamical Systems*, vol. 15 of Advanced Series in Nonlinear Dynamics, World Scientific, 2000.

[11] S. Day, J.-P. Lessard and K. Mischaikow, Validated continuation for equilibria of PDEs, *SIAM Journal on Numerical Analysis*, **45** (2007), 1398–1424.

[12] J. P. Desi, H. Edrees, J. Price, E. Sander and T. Wanner, The dynamics of nucleation in stochastic Cahn-Morral systems, *SIAM Journal on Applied Dynamical Systems*, **10** (2011), 707–743.

[13] M. Gameiro and J.-P. Lessard, Rigorous computation of smooth branches of equilibria for the three dimensional Cahn-Hilliard equation, *Numer. Math.*, **117** (2011), 753–778.

[14] M. Gameiro, J.-P. Lessard and K. Mischaikow, Validated continuation over large parameter ranges for equilibria of PDEs, *Mathematics and Computers in Simulation*, **79** (2008), 1368–1382.

[15] M. Grinfeld and A. Novick-Cohen, Counting stationary solutions of the Cahn-Hilliard equation by transversality arguments, *Proceedings of the Royal Society of Edinburgh*, **125** (1995), 351–370.

[16] A. Hungria, J.-P. Lessard and J. D. Mireles-James, Rigorous numerics for analytic solutions of differential equations: the radii polynomial approach, *Math. Comp.*, **85** (2016), 1427–1459.

[17] I. Johnson, E. Sander and T. Wanner, Branch interactions and long-term dynamics for the diblock copolymer model in one dimension, *Discrete and Continuous Dynamical Systems. Series A*, **33** (2013), 3671–3705.

[18] O. E. Lanford III, A computer-assisted proof of the Feigenbaum conjectures, *Bull. Amer. Math. Soc. (N.S.)*, **6** (1982), 427–434.

[19] J.-P. Lessard, Continuation of solutions and studying delay differential equations via rigorous numerics, *Proceedings of Symposia in Applied Mathematics*.

[20] J.-P. Lessard and J. D. Mireles James, Computer assisted Fourier analysis in sequence spaces of varying regularity, *SIAM J. Math. Anal.*, **49** (2017), 530–561.

[21] J.-P. Lessard, E. Sander and T. Wanner, Matlab codes to perform the computer-assisted proofs, Available at `http://archimede.mat.ulaval.ca/jplessard/rigbpcont/`.

[22] S. Maier-Paape, U. Miller, K. Mischaikow and T. Wanner, Rigorous numerics for the Cahn-Hilliard equation on the unit square, *Revista Matematica Complutense*, **21** (2008), 351–426.

[23] S. Maier-Paape, K. Mischaikow and T. Wanner, Structure of the attractor of the Cahn-Hilliard equation on a square, *International Journal of Bifurcation and Chaos*, **17** (2007), 1221–1263.

[24] G. Moore and A. Spence, The calculation of turning points of nonlinear equations, *SIAM Journal on Numerical Analysis*, **17** (1980), 567–576.

[25] M. T. Nakao, Numerical verification methods for solutions of ordinary and partial differential equations, *Numer. Funct. Anal. Optim.*, **22** (2001), 321–356.
[26] Y. Nishiura and I. Ohnishi, Some mathematical aspects of the micro-phase separation in diblock copolymers, *Physica D*, **84** (1995), 31–39.
[27] T. Ohta and K. Kawasaki, Equilibrium morphology of block copolymer melts, *Macromolecules*, **19** (1986), 2621—2632.
[28] M. Plum, An existence and inclusion method for two-point boundary value problems with turning points, *Z. Angew. Math. Mech.*, **74** (1994), 615–623.
[29] M. Plum, Existence and enclosure results for continua of solutions of parameter-dependent nonlinear boundary value problems, *J. Comput. Appl. Math.*, **60** (1995), 187–200.
[30] S. Rump, INTLAB - INTerval LABoratory, in *Developments in Reliable Computing* (ed. T. Csendes), Kluwer Academic Publishers, Dordrecht, 1999, 77–104.
[31] E. Sander and T. Wanner, Validated saddle-node bifurcations and applications to lattice dynamical systems, *SIAM Journal on Applied Dynamical Systems*, **15** (2016), 1690–1733.
[32] A. Spence and B. Werner, Nonsimple turning points and cusps, *IMA Journal of Numerical Analysis*, **2** (1982), 413–427.
[33] J. B. van den Berg and J.-P. Lessard, Rigorous numerics in dynamics, *Notices of the American Mathematical Society,*, **62** (2015), 1057–1061.
[34] J. B. van den Berg, J.-P. Lessard and K. Mischaikow, Global smooth solution curves using rigorous branch following, *Math. Comp.*, **79** (2010), 1565–1584.
[35] J. B. van den Berg and J. F. Williams, Validation of the bifurcation diagram in the 2d Ohta–Kawasaki problem, *Nonlinearity*, **30** (2017), 1584–1638.
[36] T. Wanner, Computer-assisted bifurcation diagram validation and applications in materials science, *Proceedings of Symposia in Applied Mathematics*, Vol. 74. American Mathematical Society, to appear.
[37] T. Wanner, Topological analysis of the diblock copolymer equation, in *Mathematical Challenges in a New Phase of Materials Science* (eds. Y. Nishiura and M. Kotani), vol. 166 of Springer Proceedings in Mathematics & Statistics, Springer-Verlag, 2016, 27–51.
[38] T. Wanner, Computer-assisted equilibrium validation for the diblock copolymer model, *Discrete and Continuous Dynamical Systems, Series A*, **37** (2017), 1075–1107.
[39] B. Werner and A. Spence, The computation of symmetry-breaking bifurcation points, *SIAM Journal on Numerical Analysis*, **21** (1984), 388–399.
[40] N. Yamamoto, A numerical verification method for solutions of boundary value problems with local uniqueness by Banach's fixed-point theorem, *SIAM J. Numer. Anal.*, **35** (1998), 2004–2013.
[41] E. Zeidler, *Nonlinear Functional Analysis and its Applications. I: Fixed-Point Theorems*, Springer-Verlag, New York – Berlin – Heidelberg, 1986.

E-mail address: jp.lessard@mcgill.ca
E-mail address: esander@gmu.edu
E-mail address: twanner@gmu.edu